Table 1 List of primers used for reverse transcription-polymerase chain reaction

Gene name	Source	Forward primer (5′→3′)		Reverse primer (3′→5′)		Product size (bp)	Cycle No
β-Actin	Mu	NM_007393 AACACCCCAGCCATGTACG	(Exon 4)	CGCTCAGGAGGAGCAATGA	(Exon 6)	623	22
	Rat	NM_031144 AACACCCCAGCCATGTACG	(Exon 4)	CGCTCAGGAGGAGCAATGA	(Exon 6)	623	18
	Hu	NM_001101 AACACCCCAGCCATGTACG	(Exon 4)	CGCTCAGGAGGAGCAATGA	(Exon 6)	623	21
EP_1	Mu	NM_013641 GACGATTCCGAAAGACCGCAG	(Exon 2)	CAACACCACCAACACCAGCAG	(Exon 2 to 3)	242	32
	Rat*	D88751 GAGAACGCAGGTCCCGATG	(Exon 1)	CCAACACCACCAATACCAGCAG	(Exon 1)	232	35
	Hu	NM_000955 GGTATCATGGTGGTGTCGTG	(Exon 2)	GGCCTCTGGTTGTGCTTAGA	(Exon 3)	317	40
EP_2	Mu	NM_008964 GATGGCAGAGGAGACGGAC	(Exon 1)	ACTGGCACTGGACTGGGTAGA	(Exon 2)	295	28
	Rat	NM_031088 TGCTCATCGTGGCTGTGCTC	(Exon 1)	GCTCTCAGTGAAGTCCGACAAC	(Exon 2)	394	35
	Hu	NM_000956 CCACCTCATTCTCCTGGCTA	(Exon 1)	CGACAACAGAGGACTGAACG	(Exon 2)	216	34
EP_3	Mu	D10204 TGCTGGCTCTGGTGGTGAC	(Exon 1)	ACTCCTTCTCCTTTCCCATCTGTG	(Exon 2)	258	30
	Rat	D14869 CCTTTGCCTCCGCCTTCG	(Exon 1)	CGAACGGCGATTAGGAAGG	(Exon 2)	313	35
	Hu	D38297 CTTCGCATAACTGGGGCAAC	(Exon 1)	TCTCCGTGTGTGTCTTGCAG	(Exon 2)	300	35
EP_4	Mu	BC011193 CTGGTGGTGCTCATCTGCTC	(Exon 2)	AGGTGGTGTCTGCTTGGGTC	(Exon 3)	445	30
	Rat	NM_032076 GCCTCAGTGACTTTCGCCG	(Exon 1)	GCTGTGCTGAACCGTCTCTG	(Exon 2)	336	35
	Hu	NM_000958 TGGTATGTGGGCTGGCTG	(Exon 2)	GAGGACGGTGGCGAGAAT	(Exon 3)	329	35

*Rat EP_1 primers were designed to generate no amplicons from either EP_1 variant cDNA (unspliced EP_1 mRNA, Genbank D88752) or genomic DNA.[39]
Mu, mouse; Hu, human.

peroxide. Sections were counterstained with haematoxylin. As a negative control, the primary antibody was preincubated with a 16-fold (molar ratio) excess amount of the fusion protein used as the immunogen for one hour at room temperature prior to incubation of the sections.[22]

AOM induced colon tumour development in EP_3 receptor knockout mice

Male EP_3 receptor deficient homozygous mice ($EP_3^{-/-}$) and wild-type mice received AOM at a dose of 10 mg/kg body weight intraperitoneally once a week for six weeks. At 56 weeks of age, mice were sacrificed under ether euthanasia and complete autopsy was performed. After laparotomy, the entire intestines were resected and opened longitudinally, and the contents were flushed with normal saline. Using a dissection microscope, colon tumours were noted grossly for their location, number, and diameter, measured with callipers. All tumours from AOM treated mice were subjected to histological examination after routine processing and haematoxylin and eosin staining. The experimental protocol was according to the guidelines for Animal Experiments in the National Cancer Center.

Effects of ONO-AE-248 on growth of colon cancer cells

The EP_3 receptor selective agonist 16-(3-methoxymethyl)-phenyl-ω-tetranor-3,7-dithiaPGE_1 (ONO-AE-248) was chemically synthesised at Ono Pharmaceutical Co. Ltd.[23] DLD-1 and HCA-7 cells were seeded in plastic 96 well plates at a density of 2×10^3 cells per well, and grown for 24 hours with media containing 5% FBS. The EP_3 receptor selective agonist ONO-AE-248 was added daily on days 0–4, and then numbers of viable cells on day 1, 3, and 5 were measured by colorimetric assay using the cell proliferation assay reagent WST-1 (Wako Chemicals, Osaka, Japan) with a microplate reader (Bio Rad, Hercules, California, USA) at a reference wavelength of 655 nm and a test wavelength of 450 nm. Cell viability was determined as per cent of control values. Experiments were repeated three times and data were measured six times (n = 6).

5′-Aza-2′-deoxycytidine treatment

CACO-2, CW-2, DLD-1, HCA-7, and WiDr cells were seeded at a density of 5×10^4 cells/10 cm dish on day 0 and treated with 1 and 2 μM 5-aza-dC (Sigma, St Louis, Missouri, USA) on days 1, 3, and 5. After each treatment, cells were placed in fresh media and harvested on day 6, and total cellular RNA was prepared using Isogen on day 7.

Statistical analysis

The significance of differences in the incidences of tumours was analysed using the χ^2 test and other differences using the Student's t test. Differences were considered statistically significant at $p<0.05$.

RESULTS

Different expression of PGE_2 receptors EP_1, EP_2, EP_3, and EP_4 in normal colon mucosa and colon tumours

Expression of PGE_2 receptors EP_1, EP_2, EP_3, and EP_4 in normal colon mucosa and colon tumours of AOM treated mice and rats, and in human tissues, were examined by RT-PCR (figs 1, 2). In the three mouse colon adenocarcinomas tested, expression of EP_1 and EP_2 receptor mRNAs was increased compared with levels in normal mucosa. EP_4 mRNA was equally expressed in carcinomas and normal mucosa. In contrast, expression of EP_3 mRNA was markedly decreased in all carcinoma samples compared with normal colon mucosa (fig 1A). Expression patterns of EP_1, EP_2, EP_3,

Table 2 List of primers used for real time reverse transcription-polymerase chain reaction

Gene name		Primer sequences (5′→3′)			Product size (bp)	Cycle condition
β-Actin	Mu, Rat, Hu	Forward	CTACAATGAGCTGCGTGTG	(Exon 3)	122	95°C (20 s) → 60°C (20 s) → 72°C (10 s)
		Reverse	TGGGGTGTTGAAGGTCTC	(Exon 4)		
EP_3	Mouse	Forward	GCTGTCCGTCTGTTGGTC	(Exon 1)	100	95°C (3 s) → 60°C (20 s)
		Reverse	CCTTCTCCTTTCCCATCTG	(Exon 2)		
	Rat	Forward	ACTGTCCGTCTGCTGGTC	(Exon 1)	100	95°C (3 s) → 60°C (20 s)
		Reverse	CCTTCTCCTTTCCCATCTG	(Exon 2)		
	Human	Forward	GTGCTGTCGGTCTGCTG	(Exon 1)	102	95°C (3 s) → 66°C (20 s)
		Reverse	CTTTCTGCTTCTCCGTGTG	(Exon 2)		

Mu, mouse; Hu, human.

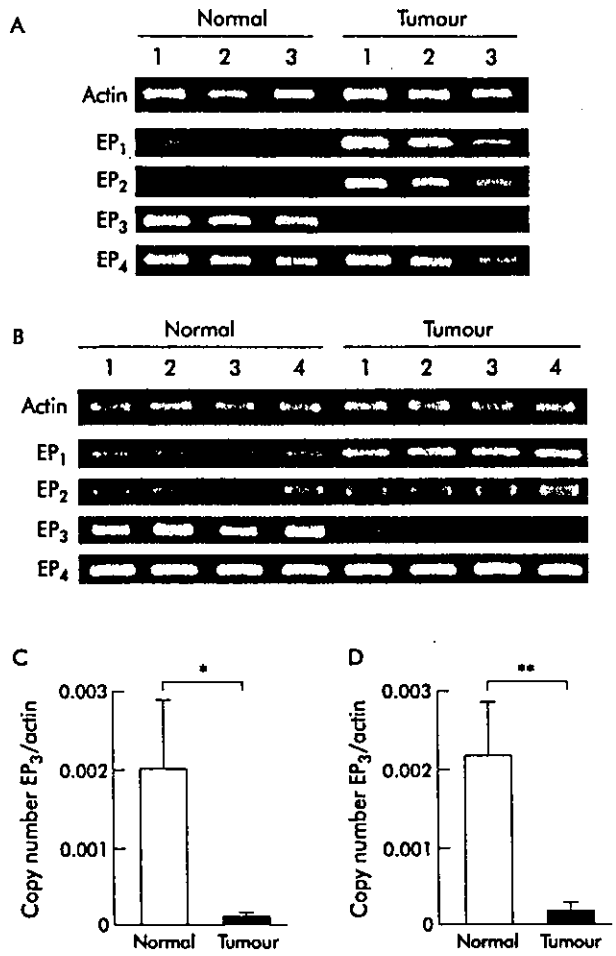

Figure 1 Analyses of prostaglandin E_2 (PGE_2) receptors EP_1, EP_2, EP_3, and EP_4 mRNA expression. (A) Azoxymethane (AOM) treated mouse normal colon mucosa and colon carcinomas. Two pairs of samples (lanes 1, 2) and two independent samples (lane 3) were examine by reverse transcription-polymerase chain reaction (RT-PCR). (B) AOM treated rat normal colon mucosa and colon carcinomas. Four pairs of samples (lanes 1–4) were examined by RT-PCR. Expression levels of EP_3 receptor mRNA were markedly lower in adenocarcinomas than in normal mucosa in all cases. (C, D) Quantitative real time RT-PCR analysis revealed significant downregulation of EP_3 receptor mRNA in AOM treated mice (C) and rat (D) colon carcinomas compared with normal colon mucosa (mouse, n=3; rat, n=4). EP_3 receptor mRNA expression was downregulated in tumours, being 5% in the mouse and 9% in the rat of the average value of that in the respective normal colon mucosa. Values are mean (SD); *p<0.05, **p<0.01. (A–D) β-Actin was used as an internal control. PCR primers of mouse and rat EP_3 receptors were designed to target a sequence common to all EP_3 receptor variants expressed in each species.

and EP_4 receptors in eight pairs of samples of adenocarcinoma and normal mucosa from AOM treated rats were similar to those in mice. Patterns for EP_1, EP_2, EP_3, and EP_4 receptors in four typical pairs of samples are shown in fig 1B. In the case of human colon tissues, EP_3 receptor mRNA was markedly decreased in seven of eight samples for adenocarcinomas compared with adjacent normal mucosa of the colon. Expression levels of EP_2 receptor mRNA were increased in seven of eight human colon adenocarcinomas compared with levels in normal mucosa, but expression of EP_1 receptor was not clearly increased in human colon carcinoma. EP_4 mRNA was equally expressed in carcinomas and normal mucosa in all cases. Figure 2A shows expression of EP_1, EP_2, EP_3, and EP_4 receptors of colon carcinoma and normal mucosa in four typical pairs of samples.

Furthermore, downregulation of EP_3 was confirmed by quantitative real time RT-PCR (figs 1C, 1D, 2B, 2C).

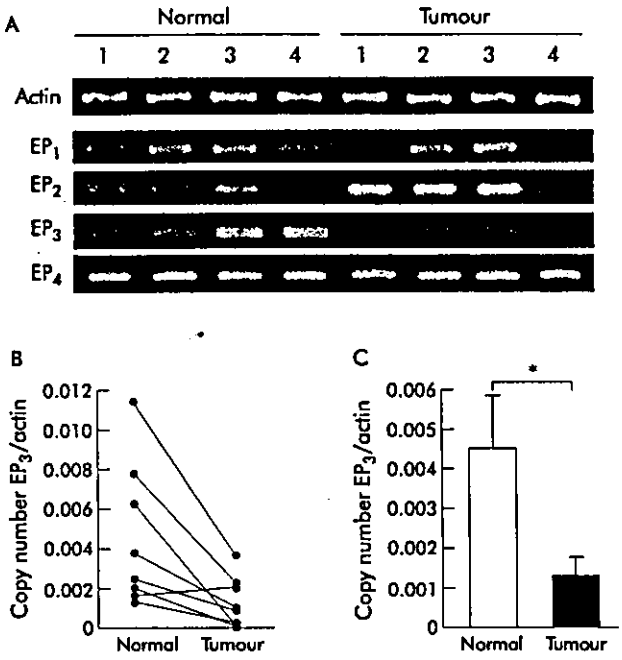

Figure 2 Analyses of prostaglandin E_2 (PGE_2) receptors EP_1, EP_2, EP_3, and EP_4 mRNA expression in human colon tissues. (A) Reverse transcription-polymerase chain reaction (RT-PCR) analysis patterns in four typical pairs of samples (lanes 1–4) are shown. (B, C) Quantitative real time RT-PCR analysis revealed significant downregulation in EP_3 receptor mRNA. (B) EP_3 receptor mRNA was markedly decreased in seven of eight samples of adenocarcinomas compared with adjacent normal mucosa of the colon. (C) EP_3 receptor mRNA expression was downregulated in tumours, being 28% of the average value of that in adjacent normal colon mucosa. Values are mean (SD); *p<0.05. (A–C) β-Actin was used as an internal control. PCR primers of human EP_3 receptors were designed to target a sequence common to all EP_3 receptor variants expressed.

Expression of EP_3 receptor mRNA was significantly downregulated in tumours, being 5% in mice (fig 1C), 9% in rats (fig 1D), and 28% in humans (fig 2C) of the average value of that in the respective normal colon mucosa.

Localisation of EP_3 receptor protein in rat colon tumours

Immunohistochemical analysis of paraffin embedded specimens of eight colon tumours and normal colon mucosa in rats treated with AOM was performed. Slight background staining was widely detected in both negative controls, those stained without antirat EP_3 receptor antibody (fig 3A, B) and those stained with anti-EP_3 receptor antibody preabsorbed with fusion EP_3 receptor protein (fig 3C, D). Moreover, slight non-specific staining was detected in red blood cells. In normal colon mucosa tissues, EP_3 receptor expression was prominent in epithelial cells (fig 3E), and the muscular coat was also positively stained. Similarly, positive staining of EP_3 receptors was observed in hyperplastic ACF of the colon (data not shown). In contrast, staining was very faint, minimal, or absent in epithelial cells of colon adenocarcinomas (fig 3F), being totally lacking in seven cases, sized 3–9 mm in diameter. Only one carcinoma sample was weakly stained, and its size was 2 mm.

Colon tumour development in EP_3 receptor knockout mice

To assess the role of EP_3 receptors in colon tumour development, EP_3 receptor knockout mice were used in an in vivo model. Data for the incidence (percentage of mice with tumours) and multiplicity (number of tumours per

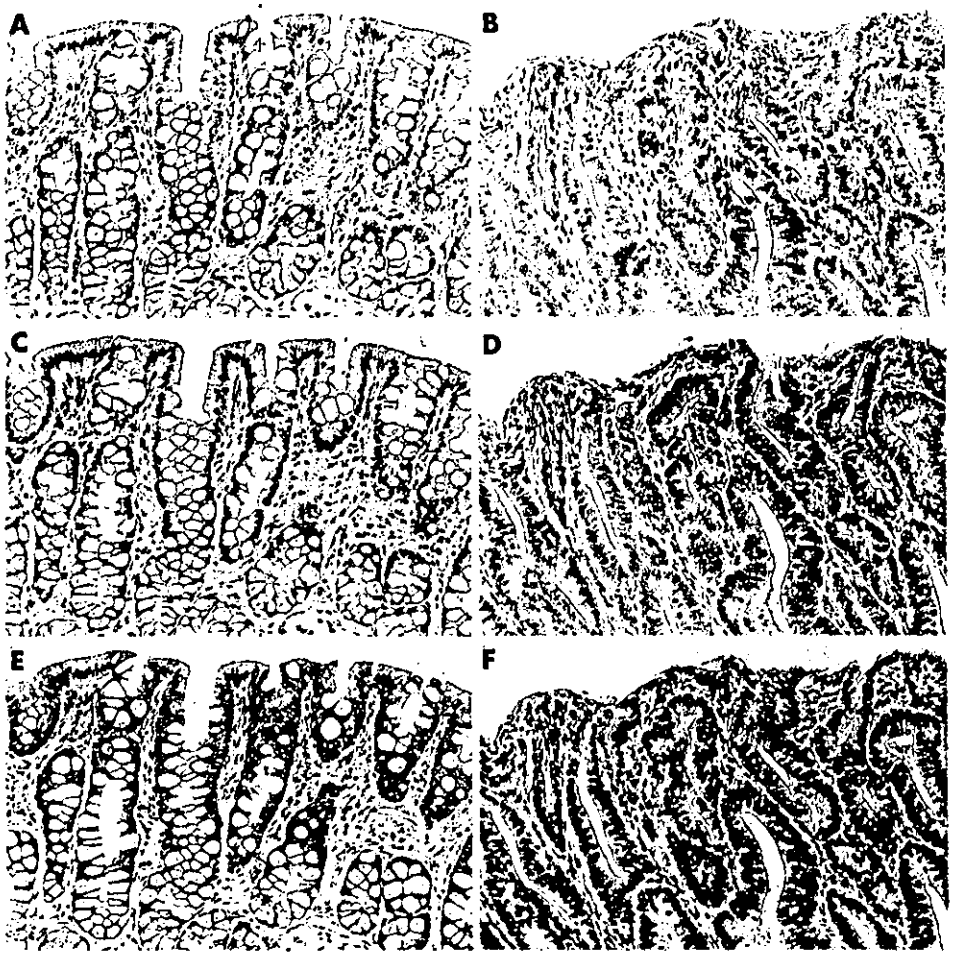

Figure 3 Immunohistochemical staining for the rat prostaglandin E_2 receptor subtype EP_3 of normal colon mucosa (A, C, and E) and colon adenocarcinoma (B, D, and F). Non-specific staining of some red blood cells and weak background staining were observed in the negative controls stained without anti-EP_3 receptor antibody (A, B) and in the negative controls stained with preabsorbed anti-EP_3 receptor antibody (C, D). With anti-EP_3 receptor antibody, immunoreactive EP_3 receptors were prominent in epithelial cells of normal colon mucosa (E) but no EP_3 receptor immunoreactivity was apparent in a colon adenocarcinoma (F). Magnification ×100.

mouse) of colon tumours induced by AOM are summarised in table 3. Tumour incidence was increased to 78% in EP_3 receptor knockout mice compared with 57% in wild-type mice. Regarding tumour multiplicity, values were 2.17 (0.51) for EP_3 receptor knockout mice and 0.75 (0.15) for wild-type mice ($p<0.05$). Histopathological examination revealed 20 colon tumours to be adenocarcinomas in wild-type, and 50 colon tumours to be three adenomas and 47 adenocarcinomas in EP_3 receptor knockout mice. Figure 4 shows the size distribution, demonstrating a significant increase in tumours measuring ≥2.0 mm in diameter in EP_3 receptor knockout mice (2.00 (0.48) *v* 0.50 (0.11); $p<0.01$) but not in those measuring <2.0 mm in diameter (0.17 (0.08) *v* 0.25 (0.11)).

Table 3 Colon tumour development in EP_3 receptor knockout mice

Mice	Incidence†	Multiplicity‡
Wild-type	16/28 (57%)	0.75 (0.15)
$EP_3^{-/-}$	18/23 (78%)	2.17 (0.51)*

†Number of mice bearing tumours per total number of mice.
‡Number of tumours per mouse. Data are mean (SEM).
Significantly different from the corresponding wild-type value ($p<0.05$).

Expressions of PGE_2 receptors in colon cancer cell lines, and effects of the EP_3 selective agonist on growth of colon cancer cells

Expression of PGE_2 receptors in 11 human colon cell lines was examined by RT-PCR. EP_1, EP_2, and EP_4 were widely detected in the human colon cancer cell lines (in 10 of 11 for EP_1, nine of 11 for EP_2, and nine of 11 for EP_4) but EP_3 was only detected in HCA-7 (fig 5A).

To evaluate the physiological functions of the EP_3 receptor, the effect of an EP_3 receptor selective agonist ONO-AE-248 on viable cell numbers of DLD-1 and HCA-7 in monolayer cultures was examined. In the HCA-7 human colon adenocarcinoma cell line, expression of the EP_3 receptor and other PGE_2 receptors (EP_1, EP_2, and EP_4) were detected by RT-PCR analysis (fig 5A). As shown in fig 5B, HCA-7 cell numbers were significantly decreased dose dependently by addition of ONO-AE-248, with 8%, 17%, and 30% decreases ($p<0.05$, $p<0.01$, and $p<0.01$) in the presence of 1, 3, and 5 μM ONO-AE-248 on day 5, respectively. On the other hand, treatment with ONO-AE-248 did not affect growth of DLD-1 cells which were not expressing EP_3 mRNA. The experiments were repeated three times and similar results were obtained.

Effect of 5-aza-dC on EP_3 expression

To determine whether silencing by DNA methylation could be involved in reduced expression of EP_3 receptor in colon tumours, we tested the effects of 5-aza-dC, a demethylating

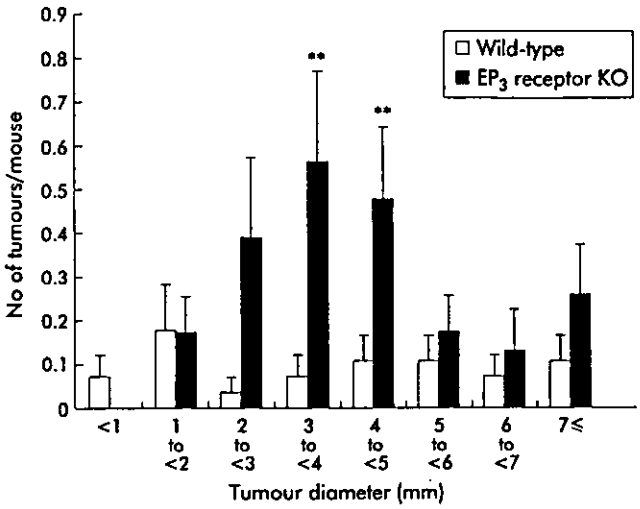

Figure 4 Size distribution of colon tumours induced by azoxymethane in wild-type and prostaglandin E_2 receptor subtype EP_3 knockout (KO) mice. The number of tumours/mouse in each size class is expressed as mean (SEM). **Significantly different from the corresponding wild-type value ($p<0.01$).

agent, on EP_3 receptor expression in colon cancer cell lines. Human colon cancer cell lines CACO-2, CW-2, DLD-1, HCA-7, and WiDr were treated with 5-aza-dC, and expression levels of EP_3 receptor were analysed by RT-PCR. Without 5-aza-dC treatment, expression of EP_3 receptor was detected in HCA-7, but not in CACO-2, CW-2, DLD-1, or WiDr (fig 5A). After 5-aza-dC treatment, expression was restored in CACO-2, CW-2, and DLD-1, but not in WiDr (fig 6).

DISCUSSION

In the present study, examination of mRNA expression levels for EP_1, EP_2, EP_3, and EP_4 receptors in colon tissues in mice, rats, and humans by RT-PCR and quantitative RT-PCR provided evidence of a marked reduction in EP_3 receptors in colon cancers, in clear contrast with the increase observed for EP_1 and EP_2. Additionally, results of mRNA expression of EP receptors in 11 human colon cancer cell lines support the above findings and further indicate the events may occur in colon cancer cells. Recently, we reported enhancement of AOM induced colon tumours with exogenous administration of PGE_2 in male F344 rats, and that colon tumours exhibited similar expression patterns in EP receptors as those observed in the present study.[24] Sonoshita *et al* reported that mRNA expression of EP_2 was strongly increased and EP_3 was weakly decreased in colon polyps compared with normal colon in *APC*$^{\Delta 716}$ mice.[19] These reports support our data that downregulation of EP_3 is a common feature in colon cancer of mice, rats, and humans. It has been reported that expression of the EP_3 receptor is widely distributed throughout the body, and its mRNA has been identified in almost all tissues in mice and rats, as well as in humans.[25–27] Northern blot analysis revealed that expression of EP_3 receptor mRNA was mainly localised in the muscle layer in the rat gastrointestinal tract,[27] and the present immunohistochemical analysis indicated that EP_3 receptors were detectable in rat normal colon epithelial cells and the muscular coat, but not in rat colon adenocarcinomas. In our previous study, we demonstrated that deficiency of EP_1 or EP_4 receptor reduced formation of AOM induced ACF while EP_3 receptors had no effect, using eight types of EP receptor knockout mice.[17 18] However, long term in vivo examination of AOM induced colon tumour development using EP_3 receptor knockout mice, conducted here in the present study, demonstrated enhancement of tumour incidence and multiplicity.

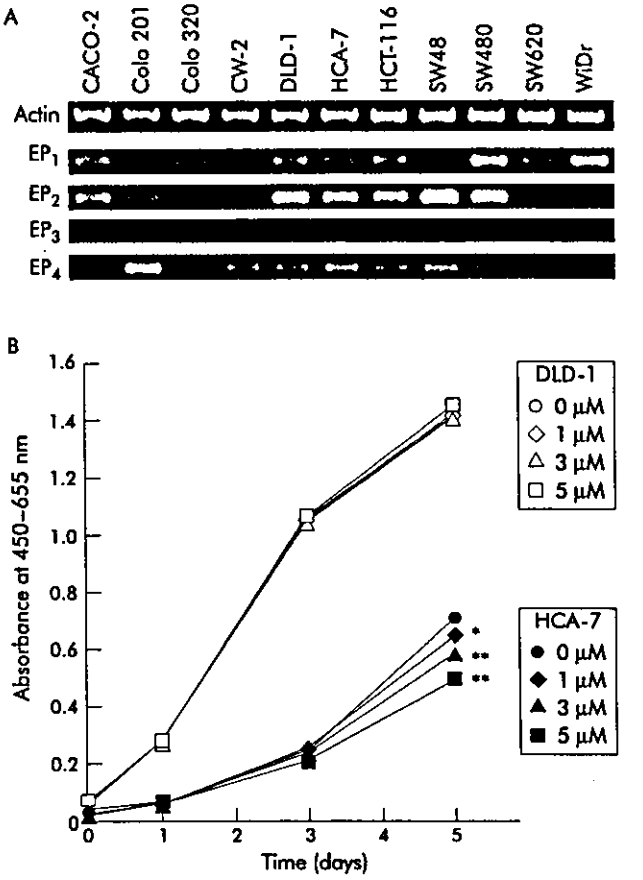

Figure 5 Effect of ONO-AE-248 treatment on cell growth of DLD-1 and HCA-7 cells. (A) Expression of prostaglandin E_2 (PGE_2) receptors EP_1, EP_2, EP_3, and EP_4 was analysed by reverse transcription-polymerase chain reaction in 11 human colon cancer cell lines. (B) DLD-1 and HCA-7 cells were seeded onto 96 well plates at a density of 2×10^3 cells/well, with media containing 5% fetal bovine serum, and treated with the EP_3 receptor selective agonist ONO-AE-248 on days 0-4. Then, cell numbers were measured by WST-1 assay on days 1, 3, and 5. Open symbols indicate DLD-1 and closed symbols HCA-7 cells; concentrations of ONO-AE-248 treatment are indicated (μM). Data are means ($n=6$). *$p<0.05$, **$p<0.01$.

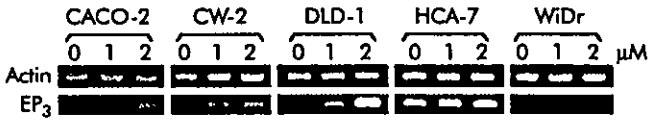

Figure 6 5-Aza-2′-deoxycytidine (5-aza-dC) treatment of CACO-2, CW-2, DLD-1, HCA-7, and WiDr colon cancer cell lines. Each cell line was treated with 1 and 2 μM 5-aza-dC three times. EP_3 receptor expression was analysed by reverse transcription-polymerase chain reaction.

Moreover, the size of the tumours was significantly increased. Thus based on our present and previous results, we suggest that the EP_3 receptor does not influence the early stage of colon carcinogenesis, including ACF formation, but its downregulation could be important to cancer development at a later stage.

In our present study, PCR primers of mouse, rat, and human EP_3 receptors targeted a common sequence in each species. PCR products would be expected to be derived from the entire range of splice variants (figs 1A–B, 2A, 5A). It is noteworthy that there are three splice variants of the EP_3 receptor in mice and rats, and nine in humans, coupled to different G protein signalling pathways.[28–33] These variants

are different in the carboxy terminal tail, and the amino acid sequence has an important role in G protein coupling specificity.[30 31] Two of the three variants of the mouse EP_3 receptors are $EP_{3\alpha}$ and $EP_{3\beta}$, which are coupled to G_i and cause inhibition of adenylate cyclase.[30] The mouse $EP_{3\gamma}$ receptor, in contrast, is coupled to G_s, in addition to G_i, and evokes pertussis toxin insensitive cAMP production.[31] Preliminarily, we examined expression of three splice variants of mouse EP_3 receptors by RT-PCR using specific primers for each variant, and found $EP_{3\alpha}$ to be the major form in mouse normal mucosa (data not shown). These observations support the conclusion that the major splice variants of EP_3 receptors are coupled to G_i and act to inhibit adenylate cyclase in normal colon mucosa in mice. On the other hand, EP_2 and EP_4 receptors are coupled to G_s and stimulate cAMP production by this enzyme. Increased cAMP levels result in activation of cAMP dependent protein kinase (PKA) and transcriptional factors that bind to cAMP responsive elements to transactivate the transcription of specific primary response genes that initiate cell proliferation.[34] In our previous study,[18] the EP_4 receptor selective agonist ONO-AE1-329 was shown to enhance colony formation by the HCA-7 human colon adenocarcinoma cell line. The EP_3 receptor selective agonist ONO-AE-248 was demonstrated to suppress cell growth in HCA-7 in the present study. It has been reported that ONO-AE-248 attenuates the rise in intracellular cAMP induced by forskolin, an activator of adenylate cyclase, in CHO cells transfected with $EP_{3\alpha}$ receptor.[23] Therefore, the EP_3 receptor pathway may play an important role in counteracting the effects of EP_2 and EP_4 receptors, and its downregulation in later stages of colon carcinogenesis may enhance cancer development. Additional studies are needed to investigate interactions between the EP_3 receptor signalling pathway and others linked to EP receptors.

Hypermethylation of CpG islands in promoter regions is known to cause silencing of genes in various human cancers,[35 36] and silencing of *COX-2* and *APC* genes by hypermethylation has been reported in human colon cancer.[37 38] Although hypermethylation of the prostaglandin receptor gene has not been reported,[37 38] DNA sequences in the promoter region and exon 1 of the human EP_3 gene are GC rich (Genbank AL031429). Therefore, in the present study, we examined the effects of demethylation of DNA with 5-aza-dC on EP_3 expression in human colon cancer cell lines. Demethylation of five cell lines by 5-aza-dC treatment resulted in restoration of EP_3 receptor expression in three cell lines. These findings suggest that the DNA sequence of the EP_3 receptor may be methylated but further studies are needed to clarify whether hypermethylation of the EP_3 receptor gene occurs and regulates EP_3 expression in colon cancers.

In conclusion, data obtained in our present and previous studies suggest that the PGE_2 receptor subtype EP_3 plays an important role in suppression of cell growth and that its downregulation enhances colon carcinogenesis at a later stage. The underlying mechanisms clearly warrant further investigation.

ACKNOWLEDGEMENTS

This work was supported in part by Grants-in-Aid for Cancer Research, for the Second-Term Comprehensive 10-Year Strategy for Cancer Control, and for the Research on Advanced Medical Technology from the Ministry of Health, Labor and Welfare of Japan.

Authors' affiliations
Y Shoji, M Takahashi, T Kitamura, K Watanabe, T Kawamori, T Sugimura, K Wakabayashi, Cancer Prevention Basic Research Project, National Cancer Center Research Institute, Tokyo, Japan
T Maruyama, Minase Research Institute, Ono Pharmaceutical Co. Ltd, Osaka, Japan
Y Sugimoto, Department of Physiological Chemistry, Faculty of Pharmaceutical Sciences, Kyoto University, Kyoto, Japan
M Negishi, Laboratory of Molecular Neurobiology, Graduate School of Biostudies, Kyoto University, Kyoto, Japan
S Narumiya, Department of Pharmacology, School of Medicine, Kyoto University, Kyoto, Japan

REFERENCES

1 **Elder DJE**, Paraskeva C. COX-2 inhibitors for colorectal cancer. *Nat Med* 1998;4:392–3.
2 **Reddy BS**, Rao CV, Rivenson A, *et al.* Inhibitory effect of aspirin on azoxymethane-induced colon carcinogenesis in F344 rats. *Carcinogenesis* 1993;14:1493–7.
3 **Rao CV**, Rivenson A, Simi B, *et al.* Chemoprevention of colon carcinogenesis by sulindac, a nonsteroidal anti-inflammatory agent. *Cancer Res* 1995;55:1464–72.
4 **Fukutake M**, Nakatsugi S, Isoi T, *et al.* Suppressive effects of nimesulide, a selective inhibitor of cyclooxygenase-2, on azoxymethane-induced colon carcinogenesis in mice. *Carcinogenesis* 1998;19:1939–42.
5 **Labyle D**, Fischer D, Vielh P, *et al.* Sulindac causes regression of rectal polyp in familial adenomatous polyposis. *Gastroenterology* 1991;101:635–9.
6 **Giardiello FM**, Hamilton SR, Krush AJ, *et al.* Treatment of colonic and rectal adenomas with sulindac in familial adenomatous polyposis. *N Engl J Med* 1993;328:1313–16.
7 **Hirata K**, Itoh H, Ohsato K. Regression of rectal polyps by indomethacin suppository in familial adenomatous polyposis. Report of two cases. *Dis Colon Rectum* 1994;37:943–6.
8 **Hirota C**, Iida M, Aoyagi K, *et al.* Effect of indomethacin suppositories on rectal polyposis in patients with familial adenomatous polyposis. *Cancer* 1996;78:1660–5.
9 **Eberhart EC**, Dubois NR. Eicosanoids and the gastrointestinal tract. *Gastroenterology* 1995;109:285–301.
10 **Kitamura T**, Kawamori T, Uchiya N, *et al.* Inhibitory effects of mofezolac, a cyclooxygenase-1 selective inhibitor, on intestinal carcinogenesis. *Carcinogenesis* 2002;23:1463–6.
11 **Narumiya S**, Sugimoto Y, Ushikubi F. Prostanoid receptors: structures, properties, and functions. *Physiol Reviews* 1999;79:1193–226.
12 **Hirai H**, Tanaka K, Yoshie O, *et al.* Prostaglandin D_2 selectively induces chemotaxis in T helper type 2 cells, eosinophils, and basophils via seven-transmembrane receptor CRTH2. *J Exp Med* 2001;93:255–61.
13 **Yang VW**, Shields JM, Hamilton SR, *et al.* Size-dependent increase in prostanoid levels in adenomas of patients with familial adenomatous polyposis. *Cancer Res* 1998;58:1750–3.
14 **Rigas B**, Goldman IS, Levine L. Altered eicosanoid levels in human colon cancer. *J Lab Clin Med* 1993;122:518–23.
15 **Pugh S**, Thomas GA. Patients with adenomatous polyps and carcinomas have increased colonic mucosal prostaglandin E_2. *Gut* 1994;35:675–8.
16 **Hasegawa H**, Negishi M, Katoh H, *et al.* Two isoforms of prostaglandin EP_3 receptor exhibiting constitutive activity and agonist-dependent activity in Rho-mediated stress fiber formation. *Biochem Biophys Res Commun* 1997;234:631–6.
17 **Watanabe K**, Kawamori T, Nakatsugi S, *et al.* Role of the prostaglandin E receptor subtype EP_1 in colon carcinogenesis. *Cancer Res* 1999;59:5093–6.
18 **Mutoh M**, Watanabe K, Kitamura T, *et al.* Involvement of prostaglandin E receptor subtype EP_4 in colon carcinogenesis. *Cancer Res* 2002;62:28–32.
19 **Sonoshita M**, Takaku K, Sasaki N, *et al.* Acceleration of intestinal polyposis through prostaglandin receptor EP_2 in $Apc^{\Delta 716}$ knockout mice. *Nat Med* 2001;7:1048–51.
20 **Takahashi M**, Fukuda K, Ohata T, *et al.* Increased expression of inducible and endothelial constitutive nitric oxide synthases in rat colon tumors induced by azoxymethane. *Cancer Res* 1997;57:1233–7.
21 **Kirkland SC.** Dome formation by a human colonic adenocarcinoma cell line (HCA-7). *Cancer Res* 1985;45:3790–5.
22 **Nakamura K**, Kaneko T, Yamashita Y, *et al.* Immunocytochemical localization of prostaglandin EP_3 receptor in the rat hypothalamus. *Neurosci Lett* 1999;260:117–20.
23 Zacharowski K, Olbrich A, Piper J, *et al* Selective activation of prostanoid EP_3 receptor reduces myocardial infarct size in rodents. *Arterioscler Thromb Vase Biol* 1999;19:2141–7.
24 **Kawamori T**, Uchiya N, Sugimura T, *et al.* Enhancement of colon carcinogenesis by prostaglandin E_2 administration. *Carcinogenesis* 2003;24:985–90.
25 **Sugimoto Y**, Namba T, Honda A, *et al.* Cloning and expression of a cDNA for mouse prostaglandin E receptor EP_3 subtype. *J Biol Chem* 1992;267:6463–6.
26 **Kotani M**, Tanaka I, Ogawa Y, *et al.* Molecular cloning and expression of multiple isoforms of human prostaglandin E receptor EP_3 subtype generated by alternative messenger RNA splicing: Multiple second messenger systems and tissue-specific distributions. *Mol Pharmacol* 1995;48:869–79.
27 **Ding M**, Kinoshita Y, Kishi K, *et al.* Distribution of prostaglandin E receptors in the rat gastrointestinal tract. *Prostaglandins* 1997;53:199–216.
28 **Kotani M**, Tanaka I, Ogawa Y, *et al.* Structural organization of the human prostaglandin EP_3 receptor subtype gene (PTGER3). *Genomics* 1997;40:425–34.
29 **Goureau O**, Tanfin Z, Marc S, *et al.* Diverse prostaglandin receptors activate distinct signal transduction pathways in rat myometrium. *Am J Physiol* 1992;263:C257–65.

30 **Sugimoto Y**, Negishi M, Hayashi Y, *et al.* Two isoforms of the EP_3 receptor with different carboxyl-terminal domains. *J Biol Chem* 1993;**268**:2712–18.
31 **Irie A**, Sugimoto Y, Namba T, *et al.* Third isoform of the prostaglandin-E-receptor EP_3 subtype with different c-terminal tail coupling to both stimulation and inhibition of adenylate cyclase. *Eur J Biochem* 1993;**217**:313–18.
32 **Takeuchi K**, Takahashi N, Abe T, *et al.* Functional difference between two isoforms of rat kidney prostaglandin receptor EP_3 subtype. *Biochem Biophys Res Commun* 1994;**203**:1897–903.
33 **Neuschafer-Rube F**, DeVries C, Hanecke K, *et al.* Molecular cloning and expression of a prostaglandin EP_3 beta subtype from rat hepatocytes. *FEBS Lett* 1994;**351**:119–22.
34 **Dhanasekaran N**, Tsim ST, Dermott JM, *et al.* Regulation of cell proliferation by G proteins. *Oncogene* 1998;**17**:1383–94.
35 **Baylin SB**, Herman JD. DNA hypermethylation in tumorigenesis: epigenetic joins genetics. *Trends Genet* 2000;**16**:168–74.
36 **Jones PA**, Laird PW. Cancer epigenetics comes of age. *Nat Genet* 1999;**21**:163–7.
37 **Esteller M**, Sparks A, Toyota M, *et al.* Analysis of adenomatous polyposis coli hypermethylation in human cancer. *Cancer Res* 2000;**60**:4366–71.
38 **Toyota M**, Shen L, Ohe-Toyota M, *et al.* Aberrant methylation of the cyclo-oxygenase 2 CpG island in colorectal tumors. *Cancer Res* 2000;**60**:4044–8.
39 **Okuda-Ashitaka E**, Sakamoto K, Ezashi T, *et al.* Suppression of prostaglandin E receptor signaling by the variant from of EP_1 subtype. *J Biol Chem* 1996;**271**:31255–61.

BMJ Publishing Group
BMA House, Tavistock Square, London WC1H 9JR. Tel. 020 7383 6305. Fax 020 7383 6699.

Printed in Great Britain by Meridian Print Centre Ltd. Derby. SJ/GUT/160/04

Cloning of Mongolian gerbil cDNAs encoding inflammatory proteins, and their expression in glandular stomach during *H. pylori* infection

Satoshi Matsubara,[1,2] Hideyuki Shibata,[2] Mami Takahashi,[1] Fumiyasu Ishikawa,[2] Teruo Yokokura,[2] Takashi Sugimura[1] and Keiji Wakabayashi[1,3]

[1]Cancer Prevention Basic Research Project, National Cancer Center Research Institute, 5-1-1 Tsukiji, Chuo-ku, Tokyo 104-0045; and [2]Yakult Central Institute for Microbiological Research, 1796 Yaho, Kunitachi-shi, Tokyo 186-8650

(Received June 29, 2004/Revised August 23, 2004/Accepted August 24, 2004)

Mongolian gerbils are considered to be a good animal model for understanding the development of *Helicobacter pylori*-associated diseases. However, limitations regarding the genetic information available for this animal species hamper the elucidation of underlying mechanisms. Thus, we have focused on identifying the nucleotide sequences of cDNAs encoding Mongolian gerbil inflammatory proteins, such as interleukin-1 (IL-1β), tumor necrosis factor α (TNF-α), cyclooxygenase-2 (COX-2) and inducible nitric oxide synthase (iNOS). Furthermore, we examined the mRNA expression of these genes in the glandular stomach by RT-PCR at 1–8 weeks after *H. pylori* infection. The deduced amino acid homologies to mouse, rat and human proteins were 86.2%, 83.6% and 67.8% for IL-1β, 87.2%, 85.1% and 78.4% for TNF-α, 91.9%, 90.2% and 84.8% for COX-2 and 90.8%, 89.1% and 80.1% for iNOS, respectively. The average stomach weight of Mongolian gerbils inoculated with *H. pylori* was increased in a time-dependent manner at 1, 2, 4 and 8 weeks after inoculation. In the pyloric region, mRNA expression levels of IL-1β, TNF-α and iNOS were increased in *H. pylori*-infected animals at the 2 weeks time point, while in the fundic region, expression levels of IL-1β, TNF-α and iNOS were elevated at 4 and 8 weeks. The COX-2 expression level in the fundic region was clearly elevated in infected animals compared with control animals at 4 and 8 weeks, but in the pyloric region, expression levels were similar in both infected and control animals. Thus, our results indicate that oxidative stress occurs from an early stage of *H. pylori* infection in the glandular stomach of Mongolian gerbils. (Cancer Sci 2004; 95: 798–802)

It is known that *Helicobacter pylori* infection is associated with upper gastrointestinal diseases, such as peptic and duodenal ulcers,[1–3] as well as gastric cancer development.[4–6] Mongolian gerbils can be readily colonized by *H. pylori*, with associated development of chronic gastritis, gastric ulcers and intestinal metaplasia after prolonged infection.[7,8] Furthermore, it has been reported that *H. pylori* infection greatly enhances *N*-methyl-*N*-nitrosourea-induced stomach carcinogenesis in Mongolian gerbils.[9] Thus, they have been used as an animal model for development of *H. pylori*-associated diseases. However, genetic information about Mongolian gerbils is relatively limited, which hampers elucidation of the underlying mechanisms.

H. pylori infection is associated with activation and infiltration of monocytes, neutrophils and lymphocytes, which produce various inflammatory factors. Inflammatory cytokines, such as interleukin-1β (IL-1β) and tumor necrosis factor α (TNF-α) are potent inhibitors of gastric acid secretion,[10,11] and the acid secretion level in turn influences *H. pylori* colonization and development of gastritis.[12] In epidemiological studies, IL-1β polymorphisms have been found to be related to gastric cancer risk.[13,14] Prostaglandins, which are synthesized from arachidonic acid by cyclooxygenases (COXs), are associated with protection of gastric mucosa.[15] There are two isomers of COX, COX-1, which is constitutively expressed, and COX-2, which is induced by various cytokines, gastric injury[16] and *H. pylori* infection.[17,18] It has also been reported that COX-2 plays an important role in the recovery from gastric ulceration.[16,17] Activated monocytes and neutrophils produce reactive oxygen species such as superoxide anion radicals, hydrogen peroxide and subsequently hydroxyl radicals in gastric mucosa.[19] The inducible nitric oxide synthase (iNOS), which is upregulated by inflammatory stimuli, produces large amounts of NO,[20] which reacts with oxygen and superoxide and produces nitrogen oxides and peroxynitrite, respectively, and these radicals are potentially genotoxic oxidants with oxidizing, nitrating and nitrosating activities.

From these observations, it seems that expression of inflammatory-associated genes, including IL-1β, TNF-α, COX-2 and iNOS, might be closely related with gastric lesions and cancer development, and it is important to analyze changes in their expression in *H. pylori*-induced gastritis. In the present study, we therefore identified the nucleotide sequences of cDNAs encoding Mongolian gerbil inflammatory factors, IL-1β, TNF-α, COX-2, iNOS, as well as β-actin (a house-keeping gene). Furthermore, we examined the mRNA expressions of these genes in the glandular stomach at 1–8 weeks after *H. pylori* infection. Based on the data obtained, the roles of IL-1β, TNF-α, COX-2, and iNOS in *H. pylori*-induced gastritis are discussed.

Materials and Methods

Bacteria. *H. pylori* (ATCC 43504; American Type Culture Collection, Manassas, VA) was grown in brucella broth supplemented with 10% heat-inactivated horse serum for 24 h at 37°C under microaerobic conditions (5% O_2, 10% CO_2 and 85% N_2), as previously described.[21]

Cell culture. Macrophages were isolated from the peritoneal cavity after injection of 5 ml aliquots of 3% proteose peptone solution into male Mongolian gerbils of 10 weeks of age (Seac Yoshitomi, Ltd., Fukuoka, Japan). After 3 days, the peritoneal cavity was washed with 15 ml of cold Hank's balanced salt solution without calcium and magnesium. The peritoneal exudate cells were collected by centrifugation and the macrophage fraction was purified by the Percoll gradient method.[22] The isolated macrophages were plated onto 24-well plates (1.0×10^6 cells/well) and maintained in RPMI 1640 medium (Gibco Industries, Inc., Langley, OK) supplemented with 10% heat-inactivated fetal bovine serum (HyClone Laboratories, Inc., Logan, UT), antibiotics (100 μg/ml of streptomycin and 100 units/ml of penicillin) and 1 μg/ml of *Escherichia coli* lipopolysaccharide (LPS, Sigma Chemical Co., St. Louis, MO) at 37°C in 5% CO_2

[3]To whom correspondence should be addressed.
E-mail: kwakabay@gan2.ncc.go.jp

for 18 h.

cDNA cloning of inflammatory factors in Mongolian gerbils. Total RNA was isolated from LPS-stimulated macrophages for the cloning of IL-1β, TNF-α, COX-2 and β-actin, and from the glandular stomach of *H. pylori*-infected Mongolian gerbils for the cloning of iNOS using ISOGEN (Nippon Gene, Tokyo). A cross-species RT-PCR method was used to obtain Mongolian gerbil cDNA fragments. Briefly, 0.5 μg aliquots of total RNA were subjected to the reverse transcription reaction with random 9-mer primer using an RNA "LA PCR" Kit (AMV) Ver.1.1 (TaKaRa Bio, Inc., Otsu, Japan). After reverse transcription, PCR was carried out with LA *Taq* polymerase (TaKaRa Bio), according to the manufacturer's instructions. Primers for IL-1β, TNF-α, COX-2, iNOS and β-actin PCR were designed from the cDNA sequences that matched perfectly between mouse and rat. PCR amplifications were performed in a thermal cycler (Gene Amp PCR System 9600, Perkin-Elmer Applied Biosystems, Foster City, CA), with an initial denaturation (94°C for 2 min) followed by 40 cycles of denaturation at 94°C for 30 s, annealing at optimum temperature for 30 s and extension at 72°C for 1 min, with a final extension process for 5 min. The PCR products were electrophoresed on 2% agarose gels, and the amplified DNA fragments were eluted and subjected to direct DNA sequencing using an "ABI PRISM" "BigDye" Terminator Cycle Sequencing Ready Reaction Kit and an ABI 310 PRIZM DNA Sequencer (PE Applied Biosystems, Foster City, CA). Mongolian gerbil-specific primers were designed from these identified sequences and rapid amplification of cDNA ends (RACE) was employed to identify the sequences of 5′ and 3′-ends. The 5′-RACE was carried out with a modified lock-docking oligo(dT) primer using a "SMART" RACE cDNA Amplification Kit (Clontech Laboratories, Inc., Palo Alto, CA).[23] Then, nested PCR was carried out with Mongolian gerbil-specific primers and nested primer in the RACE kit, and the amplified products were subjected to sequence analysis. The 3′-RACE was carried out with Mongolian gerbil-specific primers and oligo(dT) primers (Clontech, TaKaRa Bio and Invitrogen, Carlsbad, CA).

Subsequent analysis of sequence data was performed with the GENETYX software package (Genetyx Co., Tokyo).

***H. pylori* infection of Mongolian gerbils.** Specific pathogen-free male Mongolian gerbils (Seac Yoshitomi, Ltd.), 6 weeks old, were housed in an air-conditioned biohazard room with a 12 h light-dark cycle. The animals were handled according to the guidelines of the Committee for Ethics of Animal Experimentation in the National Cancer Center, Tokyo. They were fed a normal diet (CE-2; Clea Japan, Inc., Tokyo) and water *ad libitum* throughout the experimental period. At 7 weeks of age, the animals were divided into control and *H. pylori* infection groups, and each animal was fasted for 24 h. Then, *H. pylori* (0.5 ml, 2.4×10^8 CFU/ml) was orally inoculated by gavage to the animals in the *H. pylori* infection group. Control animals received sterilized broth alone. After inoculation, each animal was kept without food and drinking water for 4 h. Five animals of each group were sacrificed under ether anesthesia at 2 days, 1, 2, 4 and 8 weeks after bacterial inoculation and their stomachs were resected, opened along the greater curvature, and washed with saline twice to remove the gastric content and mucus. Then, the wet weights of the stomach and features of macroscopic gastritis were recorded. The stomachs were divided into right and left parts, and the right part was subjected to *H. pylori* detection. Pieces of the pyloric and fundic regions in the left part were subjected to RNA extraction for RT-PCR (n=3). The residue of the left part was formalin-fixed and embedded in paraffin for histological observation. Pathological diagnosis of gastritis was made according to the criteria described previously,[24,25] with a microscopic score varying from 0 to 7.

Detection of *H. pylori* colonization in the gastric mucosa. To detect *H. pylori* colonization, the glandular stomach was separated into fundic and pyloric regions, and mucosa of each region was scraped off and homogenized with 3 ml of phosphate-buffered saline. An aliquot (100 μl) of serially diluted homogenate was inoculated onto segregating agar plates for *H. pylori* (Nissui Pharmaceutical Co., Ltd., Tokyo) and incubated at 37°C under microaerobic conditions. After 5 days, the colonies were counted to determine the level of *H. pylori* colonization in each region.

mRNA expression of inflammatory factors in gastric tissue. Tissue samples from fundic and pyloric regions were immediately submerged in RNA protective solution ("RNA Later," Ambion, Austin, TX) and kept for 18 h at 4°C. Then, the tissue samples were homogenized with ISOGEN (Nippon Gene), followed by total RNA extraction. The expression levels of IL-1β, TNF-α, COX-2, iNOS and β-actin were examined by RT-PCR using Mongolian gerbil-specific primers designed from identified sequences (see Table 1 for primers and PCR conditions). The PCR products were electrophoresed on 2% agarose gels and visualized by staining with ethidium bromide.

Results

cDNA cloning of inflammatory factors in Mongolian gerbils. Cross-species RT-PCR was applied to obtain Mongolian gerbil cDNA fragments for IL-1β, TNF-α, COX-2 and β-actin from LPS-stimulated macrophages. The iNOS fragment was obtained from the glandular stomach of *H. pylori*-infected Mongolian gerbils, since no iNOS expression could be detected in LPS-stimulated macrophages. We then determined the cDNA sequences of IL-1β, TNF-α, COX-2, iNOS and β-actin of Mongolian gerbils (DDBJ/EMBL/GenBank accession number, AB177840-4). As shown in Table 2, the IL-1β, TNF-α, COX-2 and iNOS cDNAs shared more than 85% sequence homology with the mouse and rat genes, and 76.8–82.9% sequence homology to the human genes. β-Actin cDNA showed more than 90% sequence homology to mouse, rat and human β-actin. The deduced amino acid homologies to the mouse and rat proteins were in the range of 83.6–91.9%, and those to human proteins were in the range of 67.8–84.8%. The amino acid sequences of β-actin could be shown maintained more than 99% homology among Mongolian gerbil, mouse, rat and human.

Table 1. Mongolian gerbil-specific primers[1] for RT-PCR

	Forward primer (5′-3′)	Reverse primer (5′-3′)	Annealing temperature (°C)	Cycle No.[2]	Product size (bp)
IL-1β	GGCAGGTGGTATCGCTCATC	CACCTTGGATTTGACTTCTA	58	35	493
TNF-α	GCTCCCCCAGAAGTCGGCG	CTTGGTGGTTGGGTACGACA	57	40	274
COX-2	CATGGAGTGGACTTAAATCA	ATCTCTCTGCTCTGGTCAAT	53	40	699
iNOS	TCACACAGGCTGCTCCCGGC	CCATAGGAAAAGACTGCCCCG	60	35	282
β-Actin	TCCTCCCTGGAGAAGAGCTA	CCAGACAGCACTGTGTTGGC	60	30	203

1) Primers were designed from the cDNA sequences identified in this study.
2) Each cycle consisted of denaturation at 94°C for 30 s, annealing at the given temperature for 30 s and extension at 72°C for 1 min.

Table 2. The homologies of cDNA and deduced amino acid sequences of cloned Mongolian gerbil genes compared with mouse, rat and human sequences

	ORF size[1] (bp)	cDNA homology (%)			Deduced amino acid homology (%)		
		Mouse	Rat	Human	Mouse	Rat	Human
IL-1β[2]	801	88.0	87.6	76.8	86.2	83.6	67.8
TNF-α	705	86.2	85.3	81.2	87.2	85.1	78.4
COX-2	1812	89.3	89.0	82.9	91.9	90.2	84.8
iNOS	3453	89.7	89.4	82.2	90.8	89.1	80.1
β-Actin	1125	95.2	95.7	92.6	100	99.7	100

1) ORF: open reading frame.
2) cDNA sequences are registered on DDBJ/EMBL/GenBank. The accession numbers are AB177840 (IL-1β), AB177841 (TNF-α), AB177842 (COX-2), AB177843 (iNOS) and AB177844 (β-Actin).

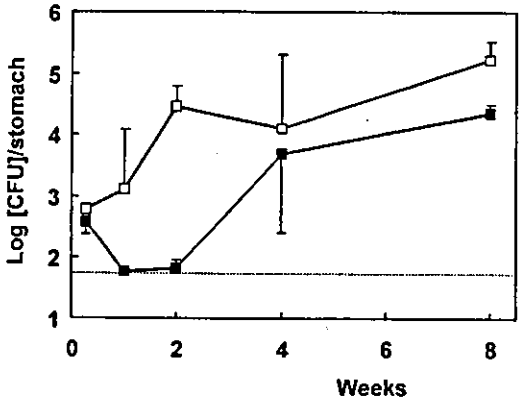

Fig. 1. The changes of *H. pylori* colonization in *H. pylori*-inoculated Mongolian gerbils. Data are mean±SD. The open squares (□) represent the values in the pyloric region and closed squares (■) represent the values in the fundic region (n=3 at 0 week and n=5 at the other weeks). The viable counts in the animal in which *H. pylori* colonization was not detected were calculated as $10^{1.78}$ CFU/stomach. The dotted line represents the detection limit (<$10^{1.78}$ CFU/stomach).

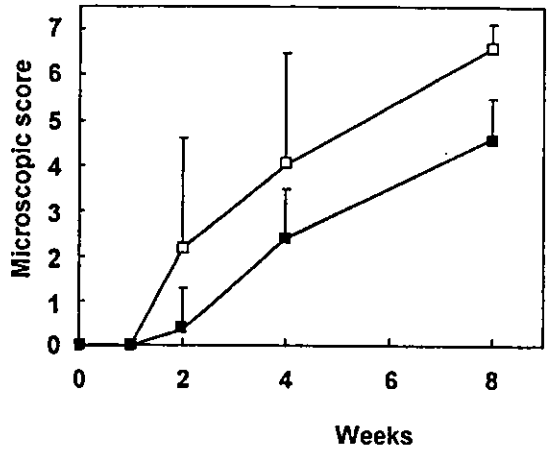

Fig. 2. The changes of pathological scores in *H. pylori*-inoculated Mongolian gerbils. Data are mean±SD. The open squares (□) represent the values in the pyloric region and closed squares (■) represent the values in the fundic region (n=3 at 0 week and n=5 at the other weeks).

Changes of gastritis parameters in *H. pylori*-infected Mongolian gerbils. Data for numbers of viable bacteria obtained from *H. pylori*-inoculated stomach samples are shown in Fig. 1. Two days after inoculation, *H. pylori* was detected in the pyloric and fundic regions of every animal, and viable counts were $10^{2.8\pm0.1}$ CFU/stomach in pyloric region and $10^{2.6\pm0.2}$ CFU/stomach in fundic region. At 1 and 2 weeks, *H. pylori* was detected in the pyloric region of every animal, and viable counts were $10^{3.1\pm0.1}$ and $10^{4.5\pm0.3}$ CFU/stomach, respectively. On the other hand, colonization was low in the fundic region, at <$10^{1.78}$ CFU/stomach in some animals. At 8 weeks, counts for *H. pylori* colonization were $10^{5.2\pm0.3}$ CFU/stomach in the pyloric region, and $10^{4.4\pm0.13}$ CFU/stomach in the fundic region.

The average stomach weights of Mongolian gerbils inoculated with *H. pylori* increased in a time-dependent manner, being 0.53±0.0, 0.62±0.1, 0.77±0.2 and 1.02±0.1 g, respectively, at 1, 2, 4 and 8 weeks after inoculation. The average stomach weights of control animals were from 0.51±0.0 to 0.52±0.0 g at 1, 2, 4 and 8 weeks. Macroscopically, gastritis with edema was observed in two of five *H. pylori*-inoculated animals at 2 weeks after inoculation, and severe gastritis with edema and hemorrhage was seen in every inoculated animal at 4 and 8 weeks. The presence of active gastritis was determined by scoring the following parameters: lymphocyte infiltration (0 to 3), polymorphonuclear leukocyte infiltration (0 to 3), and superficial erosions (0 to 1). Microscopically, erosion with infiltration, featuring many polymorphonuclear leukocytes and lymphocytes, was observed in infected animals. Fig. 2 shows the changes in pathological scores. Gastric changes were severe in the pyloric region, but moderate in the fundic region. The pathological scores at 8 weeks were 6.6±0.5 in the pyloric region and 4.6±0.9 in the fundic region. The score for animals without inoculation was 0 throughout the experimental period.

Expression of inflammatory proteins in the stomach of *H. pylori*-infected Mongolian gerbils. Total RNA was prepared from stomach tissue samples of control and *H. pylori*-infected Mongolian gerbils (n=3) at 1, 2, 4 and 8 weeks after inoculation and mRNA expression levels were assessed by RT-PCR. In the pyloric region, expression of IL-1β and TNF-α was unclear in control animals, while two of three *H. pylori*-infected animals were positive at 2 weeks, and all of the *H. pylori*-infected animals at 4 and 8 weeks (Fig. 3). In the fundic region, IL-1β and TNF-α expression levels were clearly increased in *H. pylori*-infected animals at 4 and 8 weeks. The COX-2 expression levels in the fundic region were clearly increased in infected as compared with control animals at 4 and 8 weeks, but in the pyloric region, similar expression was observed in both infected and control animals (Fig. 4). In contrast to the lack of iNOS expression in control animals, two of three *H. pylori*-infected animals were positive at 2 weeks, and the expression was markedly increased at 4 and 8 weeks in the pyloric region (Fig. 4). In the fundic region, iNOS expression was also increased in *H. pylori*-infected animals at 4 and 8 weeks. Expression levels of β-actin, evaluated as a house-keeping gene, were similar in *H. pylori*-inoculated and control animals at all time points examined (Fig. 3).

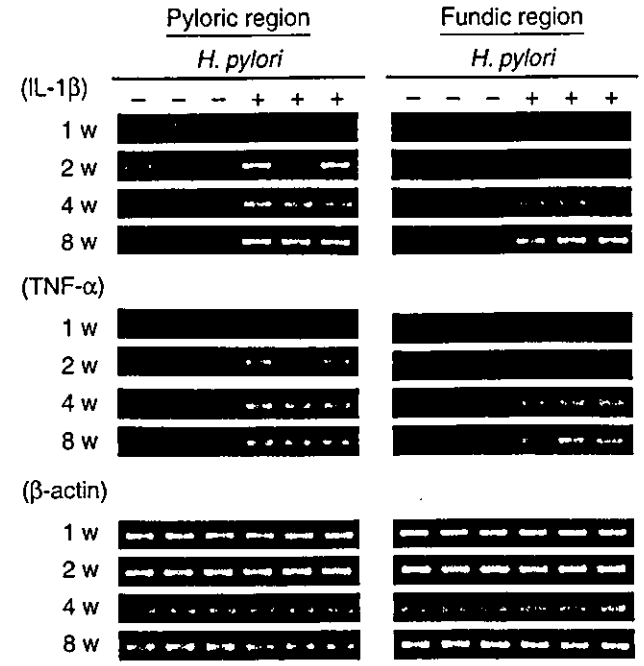

Fig. 3. Increase of IL-1β and TNF-α mRNAs in the glandular stomach of *H. pylori*-infected Mongolian gerbils. RT-PCR analysis was performed with samples from glandular stomach of control and *H. pylori*-infected animals at 1, 2, 4 and 8 weeks after inoculation. Note the similarity of expression levels of β-actin, assayed as a house-keeping gene, between *H. pylori*-inoculated and control animals. The sizes of the amplified products were determined to be 493 bp for IL-1β, 274 bp for TNF-α and 203 bp for β-actin.

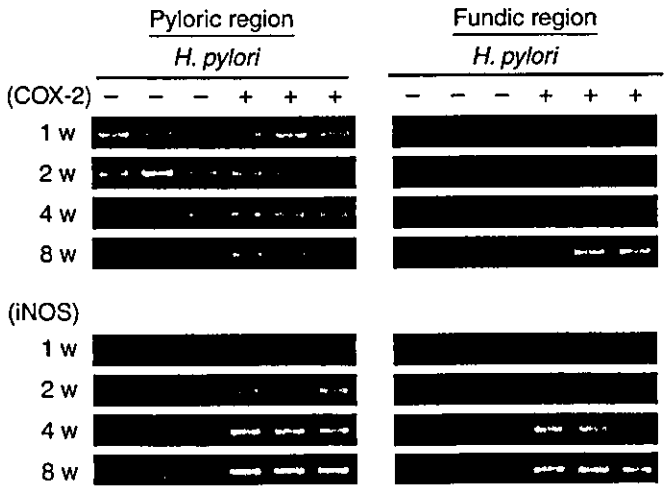

Fig. 4. Expression levels of COX-2 and iNOS mRNAs in the stomach of control and *H. pylori*-infected Mongolian gerbils. RT-PCR analysis was performed with samples from glandular stomach of control and *H. pylori*-infected animals at 1, 2, 4 and 8 weeks after inoculation. The sizes of the amplified products were 699 bp for COX-2 and 282 bp for iNOS.

Discussion

In the present study, we determined the cDNA sequences of IL-1β, TNF-α, COX-2, iNOS and β-actin in Mongolian gerbils. Partial sequences of Mongolian gerbil IL-1β, β-actin[26] and COX-2[27] have been reported earlier, and the homologies with our sequences were 99.7%, 97.6% and 99.9%, respectively. The deduced amino acid homologies of these inflammatory proteins were more than 80% among the Mongolian gerbils, mouse and rat forms. Human IL-1β consists of 269 amino acids containing a mature protein (153 amino acids), the homology of IL-1β with the Mongolian gerbils protein being higher in the mature protein (75.0%) than in the residual peptides (59.0%). TNF-α is also synthesized as a premature protein, but the homologies appear similar in the mature protein and residual peptides. It has been reported that seven amino acids (Leu105, Arg108, Leu112, Ala160, Ser162, Val167 and Glu222 in human premature TNF-α) are crucial for TNF-α activities,[28] and these amino acids were here found to be conserved in Mongolian gerbils, as in the mouse, rat and human cases. COX-2 catalyzes the synthesis of prostaglandins from arachidonic acid, and has an arachidonic acid binding domain, which consists of 24 amino acids.[29] All these were perfectly conserved in Mongolian gerbils, as in the mouse and human (rat; Ser339→Trp).

There are many reports that iNOS is induced in murine macrophages by stimulation with *E. coli* LPS.[30] However, no iNOS expression was observed in macrophages of Mongolian gerbils after LPS (1 μg/ml) treatment. Therefore, we obtained an iNOS cDNA fragment from the stomach of *H. pylori*-infected Mongolian gerbils. The active center of the iNOS oxygenase domain is Glu371 (mouse), which binds to substrate L-arginine, and Trp366, which binds to a heme.[31] These two amino acids were conserved in Mongolian gerbils, as in the mouse, rat and human forms.

It has been reported that *H. pylori* infection increases the expression of IL-1β, TNF-α, COX-2 and iNOS in clinical biopsy samples. However, data on these inflammatory proteins in the early stage of *H. pylori* infection have hitherto not been available. In the present study, expression of IL-1β, TNF-α and iNOS was observed from 2 weeks after inoculation in the pyloric region, and from 4 weeks in the fundus. The delay presumably reflects differences in *H. pylori* colonization levels in the two sites. IL-1β and TNF-α stimulate the production of reactive oxygen species from leucocytes, and iNOS produces NO. Thus, DNA damage may occur through oxidative stress from an early stage of *H. pylori* infection. Although it has been reported that COX-2 protein is not detectable in the glandular stomach of *H. pylori*-uninfected Mongolian gerbils,[18,32] in the present study, mRNA expression was observed in both control animals and infected animals. Similar results were also obtained using other COX-2-specific primer pairs (data not shown). Since these primers were designed from sequences that shared low homology with COX-1 and COX-2, it is most likely that these amplified products were not derived from COX-1 mRNA. It is reported that COX-2 expression in human normal mucosa was detected by RT-PCR, but COX-2 protein was not observed.[33] Thus, trace amounts of COX-2 mRNA in uninfected animals might be amplified and explain the discrepancy. In the present study, COX-2 mRNA expression was clearly upregulated in the fundic region, but not in the pyloric region. It is not yet clear why the expression of COX-2 mRNA was observed without development of gastritis in the pyloric region. It has been reported that COX-2 expression was observed in fibroblasts in the glandular stomach of Mongolian gerbils.[34] Therefore, it is speculated that COX-2 expression in the pyloric region of uninfected Mongolian gerbils might be derived from fibroblasts. It is also not clear why the upregulation of COX-2 mRNA was not observed in the pyloric region of *H. pylori*-infected animals. Further study is required to understand the mechanism.

The fundic and pyloric regions have very different functions. Gastric acid is secreted from the fundic region, and gastrin, which stimulates acid secretion, is secreted from the pyloric region. *H. pylori* colonization may be more difficult in the fundus because of the acid secretion.[12,35] Acid hyposecretion because of H_2 blockers or vagotomy enhances gastritis and *H. pylori*

colonization in the fundic region. Consistent with the available data, we found in the present study that gastritis developed more severely and rapidly in the pyloric region, where *H. pylori* colonization was more pronounced, particularly at 2 weeks after inoculation. IL-1β and TNF-α inhibit the secretion of gastric acid,[10,11] and *H. pylori* infection decreases acid secretion from 4 weeks after inoculation in Mongolian gerbils.[25,36] Since IL-1β and TNF-α expressions were observed from 2 weeks in the pyloric region, their expression might influence *H. pylori* infection in the fundic region through the acid hyposecretion. Indeed, *H. pylori* numbers in the fundus increased from 4 weeks after inoculation as shown in Fig. 1 in the present study.

In conclusion, cDNAs encoding the inflammatory proteins IL-1β, TNF-α and iNOS of Mongolian gerbils were cloned, and their expression levels were found to be correlated with gastritis development. Upregulation of COX-2 mRNA expression was seen in the fundic region of infected animals, while COX-2 mRNA expression in the pyloric region was observed in both infected and control animals. The observed upregulation from 2 weeks after *H. pylori* infection suggests that oxidative stresses may occur from an early stage of colonization.

We thank Naoaki Uchiya, Mika Kawamura and Yurika Teramoto for their expert technical assistance. This work was supported in part by Grants-in-Aid for Cancer Research and for the 2nd Term Comprehensive 10-Year Strategy for Cancer Control from the Ministry of Health, Labour and Welfare, Japan, and also a grant from the Yakult Bio-science Foundation.

1. Blaser MJ. Hypotheses on the pathogenesis and natural history of *Helicobacter pylori*-induced inflammation. *Gastroenterology* 1992; **102**: 720–7.
2. Forman D, Newell DG, Fullerton F, Yarnell JWG, Stacey AR, Wald N, Sitas F. Association between infection with *Helicobacter pylori* and risk of gastric cancer: evidence from a prospective investigation. *Br Med J* 1991; **302**: 1302–5.
3. Parsonnet J, Hansen S, Rodriguez L, Gelb AB, Warnke RA, Jellum E, Orentreich N, Vogelman JH, Friedman GD. *Helicobacter pylori* infection and gastric lymphoma. *N Engl J Med* 1994; **330**: 1267–71.
4. Nomura A, Stemmermann GN, Chyou PH, Kato I, Perez-Perez GI, Blaser MJ. *Helicobacter pylori* infection and gastric carcinoma among Japanese Americans in Hawaii. *N Engl J Med* 1991; **325**: 1132–6.
5. Parsonnet J, Friedman GD, Vandersteen DP, Chang Y, Vogelman JH, Orentreich N, Sibley RK. *Helicobacter pylori* infection and the risk of gastric carcinoma. *N Engl J Med* 1991; **325**: 1127–31.
6. Uemura N, Okamoto S, Yamamoto S, Matsumura N, Yamaguchi S, Yamakido M, Taniyama K, Sasaki N, Schlemper RJ. *Helicobacter pylori* infection and the development of gastric cancer. *N Engl J Med* 2001; **345**: 784–9.
7. Hirayama F, Takagi S, Yokoyama Y, Iwao E, Ikeda Y. Establishment of gastric *Helicobacter pylori* infection in Mongolian gerbils. *J Gastroenterol* 1996; **31** Suppl 9: 24–8.
8. Hirayama F, Takagi S, Kusuhara H, Iwao E, Yokoyama Y, Ikeda Y. Induction of gastric ulcer and intestinal metaplasia in Mongolian gerbils infected with *Helicobacter pylori*. *J Gastroenterol* 1996; **31**: 755–7.
9. Sugiyama A, Maruta F, Ikeno T, Ishida K, Kawasaki S, Katsuyama T, Shimizu N, Tatematsu M. *Helicobacter pylori* infection enhances *N*-methyl-*N*-nitrosourea-induced stomach carcinogenesis in the Mongolian gerbil. *Cancer Res* 1998; **58**: 2067–9.
10. Beales ILP, Calam J. Interleukin 1 beta and tumour necrosis factor alpha inhibit acid secretion in cultured rabbit parietal cells by multiple pathways. *Gut* 1998; **42**: 227–34.
11. Kondo S, Shinomura Y, Kanayama S, Kawabata S, Miyazaki Y, Imamura I, Fukui H, Matsuzawa Y. Interleukin-1 beta inhibits gastric histamine secretion and synthesis in the rat. *Am J Physiol* 1994; **267**: G966–71.
12. Furuta T, Shirai N, Takashima M, Xiao F, Sugimura H. Effect of genotypic differences in interleukin-1 beta on gastric acid secretion in Japanese patients infected with *Helicobacter pylori*. *Am J Med* 2002; **112**: 141–3.
13. El-Omar EM, Carrington M, Chow WH, McColl KE, Bream JH, Young HA, Herrera J, Lissowska J, Yuan CC, Rothman N, Lanyon G, Martin M, Fraumeni JF Jr, Rabkin CS. Interleukin-1 polymorphisms associated with increased risk of gastric cancer. *Nature* 2000; **404**: 398–402.
14. Hamajima N, Matsuo K, Saito T, Tajima K, Okuma K, Yamao K, Tominaga S. Interleukin 1 polymorphisms, lifestyle factors, and *Helicobacter pylori* infection. *Jpn J Cancer Res* 2001; **92**: 383–9.
15. Robert A, Nezamis JE, Lancaster C, Hanchar AJ. Cytoprotection by prostaglandins in rats. Prevention of gastric necrosis produced by alcohol, HCl, NaOH, hypertonic NaCl, and thermal injury. *Gastroenterology* 1979; **77**: 433–43.
16. Mizuno H, Sakamoto C, Matsuda K, Wada K, Uchida T, Noguchi H, Akamatsu T, Kasuga M. Induction of cyclooxygenase 2 in gastric mucosal lesions and its inhibition by the specific antagonist delays healing in mice. *Gastroenterology* 1997; **112**: 387–97.
17. Tatsuguchi A, Sakamoto C, Wada K, Akamatsu T, Tsukui T, Miyake K, Futagami S, Kishida T, Fukuda Y, Yamanaka N, Kobayashi M. Localisation of cyclooxygenase 1 and cyclooxygenase 2 in *Helicobacter pylori* related gastritis and gastric ulcer tissues in humans. *Gut* 2000; **46**: 782–9.
18. Takahashi S, Fujita T, Yamamoto A. Role of cyclooxygenase-2 in *Helicobacter pylori*-induced gastritis in Mongolian gerbils. *Am J Physiol Gastrointest Liver Physiol* 2000; **279**: G791–8.
19. Davies GR, Simmonds NJ, Stevens TR, Sheaff MT, Banatvala N, Laurenson IF, Blake DR, Rampton DS. *Helicobacter pylori* stimulates antral mucosal reactive oxygen metabolite production *in vivo*. *Gut* 1994; **35**: 179–85.
20. Nathan C. Inducible nitric oxide synthase: what difference does it make? *J Clin Invest* 1997; **100**: 2417–23.
21. Shibata H, Iimuro M, Uchiya N, Kawamori T, Nagaoka M, Ueyama S, Hashimoto S, Yokokura T, Sugimura T, Wakabayashi K. Preventive effects of Cladosiphon fucoidan against *Helicobacter pylori* infection in Mongolian gerbils. *Helicobacter* 2003; **8**: 59–65.
22. Hashimoto S, Nagaoka M, Hayashi K, Yokokura T, Mutai M. Role of culture supernatant of cytotoxic/cytostatic macrophages in activation of murine resident peritoneal macrophages. *Cancer Immunol Immunother* 1989; **28**: 253–9.
23. Borson ND, Salo WL, Drewes LR. A lock-docking oligo(dT) primer for 5′ and 3′ RACE PCR. *PCR Methods Appl* 1992; **2**: 144–8.
24. Rauws EAJ, Langenberg W, Houthoff HJ, Zanen HC, Tytgat GN. *Campylobacter pyloridis*-associated chronic active antral gastritis. A prospective study of its prevalence and the effects of antibacterial and antiulcer treatment. *Gastroenterology* 1988; **94**: 33–40.
25. Matsubara S, Shibata H, Ishikawa F, Yokokura T, Takahashi M, Sugimura T, Wakabayashi K. Suppression of *Helicobacter pylori*-induced gastritis by green tea extract in Mongolian gerbils. *Biochem Biophys Res Commun* 2003; **310**: 715–9.
26. Takashima M, Furuta T, Hanai H, Sugimura H, Kaneko E. Effects of *Helicobacter pylori* infection on gastric acid secretion and serum gastrin levels in Mongolian gerbils. *Gut* 2001; **48**: 765–73.
27. Sakai T, Fukui H, Franceschi F, Penland R, Sepulveda AR, Fujimori T, Terano A, Genta RM, Graham DY, Yamaoka Y. Cyclooxygenase expression during *Helicobacter pylori* infection in Mongolian gerbils. *Dig Dis Sci* 2003; **48**: 2139–46.
28. Van Ostade X, Tavernier J, Prange T, Fiers W. Localization of the active site of human tumour necrosis factor (hTNF) by mutational analysis. *EMBO J* 1991; **10**: 827–36.
29. Smith WL, DeWitt DL, Garavito RM. Cyclooxygenases: structural, cellular, and molecular biology. *Annu Rev Biochem* 2000; **69**: 145–82.
30. Wilson KT, Ramanujam KS, Mobley HLT, Musselman RF, James SP, Meltzer SJ. *Helicobacter pylori* stimulates inducible nitric oxide synthase expression and activity in a murine macrophage cell line. *Gastroenterology* 1996; **111**: 1524–33.
31. Crane BR, Arvai AS, Ghosh DK, Wu C, Getzoff ED, Stuehr DJ, Tainer JA. Structure of nitric oxide synthase oxygenase dimer with pterin and substrate. *Science* 1998; **279**: 2121–6.
32. Futagami S, Hiratsuka T, Wada K, Tatsuguchi A, Tsukui T, Miyake K, Akamatsu T, Hosone M, Sakamoto C, Kobayashi M. Inhibition of *Helicobacter pylori*-induced cyclo-oxygenase-2 aggravates NSAID-caused gastric damage in Mongolian gerbils. *Aliment Pharmacol Ther* 2002; **16**: 847–55.
33. Fu S, Ramanujam KS, Wong A, Fantry GT, Drachenberg CB, James SP, Meltzer SJ, Wilson KT. Increased expression and cellular localization of inducible nitric oxide synthase and cyclooxygenase 2 in *Helicobacter pylori* gastritis. *Gastroenterology* 1999; **116**: 1319–29.
34. Nakamura M, Takahashi S, Matsui H, Nishikawa K, Akiba Y, Ishii H. Persistent increase in myofibroblasts in *Helicobacter heilmannii*-infected mice but not in *Helicobacter pylori*-infected Mongolian gerbils: colocalization of COX-2 and bFGF immunoreactivity. *Aliment Pharmacol Ther* 2002; **16** Suppl 2: 174–9.
35. Morris A, Nicholson G. Ingestion of *Campylobacter pyloridis* causes gastritis and raised fasting gastric pH. *Am J Gastroenterol* 1987; **82**: 192–9.
36. Fukui H, Franceschi F, Penland RL, Sakai T, Sepulveda AR, Fujimori T, Terano A, Chiba T, Genta RM. Effects of *Helicobacter pylori* infection on the link between regenerating gene expression and serum gastrin levels in Mongolian gerbils. *Lab Invest* 2003; **83**: 1777–86.

Carcinogenesis vol.25 no.10 pp.1967–1972, 2004
doi:10.1093/carcin/bgh189

Carcinogenicity of aminophenylnorharman, a possible novel endogenous mutagen, formed from norharman and aniline, in F344 rats

Toshihiko Kawamori[1], Yukari Totsuka, Naoaki Uchiya, Tomohiro Kitamura, Hideyuki Shibata, Takashi Sugimura and Keiji Wakabayashi[2]

Cancer Prevention Basic Research Project, National Cancer Center Research Institute, 1-1 Tsukiji 5-chome, Chuo-ku, Tokyo 104-0045, Japan

[1]Present address: Pathology and Laboratory Medicine, Medical University of South Carolina, 165 Ashley Avenue, Suite 309, Charleston, SC 29425, USA

[2]To whom correspondence should be addressed
Email: kwakabay@gan2.res.ncc.go.jp

A novel mutagenic compound, 9-(4′-aminophenyl)-9*H*-pyrido[3,4-*b*]indole (aminophenylnorharman, APNH), is shown to be formed by the *in vitro* enzymatic reaction of 9*H*-pyrido[3,4-*b*]indole (norharman) and aniline. APNH generates DNA adducts (dG-C8-APNH), and is potently genotoxic to bacteria and mammalian cells. APNH has also been demonstrated to be formed *in vivo* from norharman and aniline, and suggested to be a new type of endogenous mutagenic compound. To determine its carcinogenic activity, long-term administration of APNH was investigated in 93 male and 90 female F344 rats. Rats were fed diets containing 0, 20 or 40 p.p.m. from 7 weeks of age. All animals were killed after 85 weeks treatment and necropsy was performed. Hepatocellular carcinomas (HCCs) were induced at incidences of 10 and 79% in male rats fed 20 and 40 p.p.m. APNH, and 34% in female rats fed 40 p.p.m. of APNH, respectively. In addition, colon adenocarcinomas were found at incidences of 3 and 9% in male rats, and 4 and 13% in female rats fed 20 and 40 p.p.m. of APNH, respectively. Other tumors, including thyroid carcinomas and mononuclear cell leukemia, were also seen in rats fed APNH. Polymerase chain reaction–single strand conformation polymorphism analysis revealed β-*catenin* gene mutations in 24% of HCCs and K-*ras*, β-*catenin* and *Apc* gene mutations were found in 22, 44 and 33% of colon cancers induced by APNH, respectively. Most mutations occurred at G:C base pairs. β-*Catenin* protein accumulations in the nucleus and cytoplasm were also revealed in both liver and colon tumors. Thus, APNH induced liver and colon cancers with K-*ras*, β-*catenin* and *Apc* gene mutations in F344 rats.

Introduction

On heating tryptophan, a β-carboline compound, 9*H*-pyrido [3,4-*b*]indole (norharman) is produced, together with mutagenic/carcinogenic heterocyclic amines (HCAs), α- and γ-carbolines (1,2). Norharman is reported to be present at much higher levels than those of HCAs in cigarette smoke condensate and cooked meat and fish (3). Furthermore, norharman is detected in all urine samples from healthy volunteers eating an ordinary diet, as well as from patients receiving parenteral alimentation (4). It has been found that norharman becomes mutagenic to *Salmonella typhimurium* TA98 with a metabolic activation system (S9 mix) when incubated with a non-mutagenic aromatic amine, aniline, although norharman itself is not mutagenic to *S.typhimurium* TA98 and TA100, either with or without an S9 mix (2,5). Aniline is also present in cigarette smoke condensate and some kinds of vegetables (6,7). Moreover, this compound has been reported to be present in human urine and milk samples (8–10). Thus, it is likely that humans are simultaneously exposed to both compounds in daily life. We have demonstrated that a mutagenic compound, 9-(4′-aminophenyl)-9*H*-pyrido[3,4-*b*]indole (aminophenylnorharman, APNH, shown in Figure 1), is formed from norharman and aniline, then converted to the *N*-hydroxyamino derivative, which produces DNA adducts after esterification to induce mutations in *S.typhimurium* TA98 and YG1024 (11–13). Recently, we clarified that APNH forms DNA adducts primarily at the C-8 position of guanine residues *in vitro* and *in vivo* (14). In addition, APNH was found to induce sister chromatid exchanges and chromosome aberrations (15). Moreover, APNH was detected in 24 h urine samples collected from F344 rats administered norharman and aniline (16).

As mentioned above, humans are exposed to both norharman and aniline, so that it is very likely that APNH may be produced in our bodies. In fact, APNH was detected in some 24 h urine samples from smokers (our unpublished data) and therefore could play an important role in human carcinogenesis as a new type of endogenous mutagen. To understand the effects of APNH on human health, it is important to elucidate its carcinogenicity in rodents. We have demonstrated previously that APNH induces glutathione *S*-transferase placental (GST-P) positive foci, pre-neoplastic hepatic lesions, in the livers of male F344 rats in a short-term experiment (17). In the present study, the carcinogenicity of APNH with long-term administration in both male and female F344 rats was investigated. Tumors were found in the liver and colon, and mutation analysis of cancer-related K-*ras*, β-*catenin*, *Apc* and *p53* genes in the lesions, was also performed using polymerase

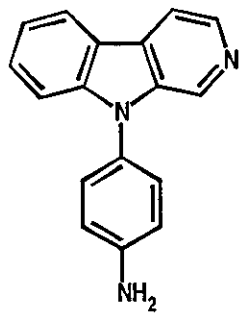

Fig. 1. Chemical structure of APNH.

Abbreviations: APNH, aminophenylnorharman, 9-(4′-aminophenyl)-9*H*-pyrido[3,4-*b*]indole; norharman, 9*H*-pyrido[3,4-*b*]indole; HCCs, hepatocellular carcinomas; IQ, 2-amino-3-methylimidazo[4,5-*f*]quinoline; PCR–SSCP, polymerase chain reaction–single strand conformation polymorphism.

P-151

chain reaction–single strand conformation polymorphism (PCR–SSCP) to give points to underlying mechanisms.

Materials and methods

Animals and chemicals

A total of 186 weanling F344 rats of both sexes were obtained from Charles River Japan (Atsugi, Japan) and quarantined for 2 weeks. All animals were housed three to a plastic cage. Rats were randomly distributed into three groups and maintained under controlled conditions: 12-h light/dark cycle, 21 ± 2°C room temperature, and 50 ± 10% relative humidity. CE-2, purchased from Japan Clea Laboratory, Tokyo, Japan, was used as the basal control diet. Food and water were available *ad libitum* throughout the experiment. APNH was purchased from the Nard Institute (Osaka, Japan) and its purity was confirmed to be >99% by HPLC.

Experimental procedure

Starting at 7 weeks of age, the rats were fed either control pellet diet (CE-2) or experimental diets containing 20 or 40 p.p.m. APNH until the termination. Body weights and diet consumption were recorded weekly during the first 14 weeks and then every 4 weeks until the end of the study. When animals were found to be moribund, they were killed and complete autopsy was performed. At 85 weeks after the beginning of the experiment, all surviving animals were killed by ether and similarly processed. Organs/tissues including brain, skin—including specialized sebaceous glands, oral cavity, esophagus, stomach, intestines, salivary glands, liver, pancreas, kidneys, urinary bladder, thyroid gland, mammary glands, lungs, spleen, thymus, bone marrow, heart, adrenal glands, pituitary gland, male reproductive system including testis, epididymis, prostate, and seminal vesicles or female reproductive system including ovary, uterus and vagina were examined under a dissection microscope for any abnormality. For histological evaluation, all organs were fixed in 10% neutral-buffered formalin, embedded in paraffin blocks, cut into multiple sections, and routinely processed for H&E staining. The histological criteria adapted for diagnoses of tumors were according to 'Pathology of the Fischer Rat' (18). Half of the liver tumors were stocked in liquid nitrogen for subsequent PCR–SSCP analyses.

PCR–SSCP analysis and direct sequencing

Genomic DNA of liver tumors was obtained from frozen tissue samples using standard procedures involving enzymatic digestion of protein and RNA followed by extraction with phenol and chloroform:isoamyl alcohol (24:1, v/v). In the colon tumors, DNA was extracted from 10 μm thick sections cut from paraffin-embedded materials with TaKaRa DEXPAT™ (TaKaRa Shuzo, Kyoto, Japan) according to the manufacturer's instructions. The primers and PCR conditions for the β-*catenin*, *Apc*, *p53* and *ras* family genes examined in this study were the same as those reported previously (19–24). One microliter of PCR products was mixed with 9 μl of 95% formamide, 20 mM EDTA, 0.05% bromophenol blue and 0.05% xylene cyanol, heated at 90°C for 3 min, then applied to a 10 or 12.5% polyacrylamide gel with or without 5% glycerol. Electrophoresis was carried out at 300 V for 2 h at 20°C and the gel was stained using a silver staining kit (Daiichi Pure Chemicals, Tokyo, Japan). When mutated shifted-bands were observed in the gels, mutation analysis was performed by direct sequencing of DNA fragments extracted from SSCP bands or PCR products using a capillary sequencer (ABI PRISM 310 Genetic Analyzer, Perkin Elmer, Foster City, CA).

Immunohistochemical staining of β-catenin

Immunohistochemical analysis was performed with the same procedure as described previously, with minor modifications (21). Briefly, after deparaffinization and re-hydration, samples were microwaved (5 min, five times) in 10 mM citrate buffer (pH 6.0), then endogenous peroxidase activity and non-specific reactions were blocked with 0.3% hydrogen peroxide and 5% normal horse serum, respectively. The sections were then incubated overnight with an anti-β-catenin monoclonal antibody diluted at 1:500 (Transduction Lab., Lexington, KY) at 4°C. Then, the sections were incubated at room temperature with the secondary antibody, biotinated anti-mouse IgG (H+L) raised in a horse, at 1:200 (Vector, Burlingame, CA) for 30 min. Staining was carried out using a Vectastain ABC kit (Vector), 3,3′-diaminobenzidine and hydrogen peroxide. All sections were counterstained with hematoxylin. The bile duct epithelium was considered as a positive control in all liver sections.

Statistical analysis

The Fisher's exact probability test was used for statistical analysis of differences in tumor incidences. Significance was concluded at $P < 0.05$.

Results

General observations

Body weights of control male rats reached 450 g, and those of female rats almost 250 g during the study. Values for male rats fed 40 p.p.m. of APNH were decreased to 95% as compared with the control group at 80 weeks ($P < 0.05$). Female rats receiving the 40 p.p.m. dose also demonstrated 5–10% lower body weights than those in the control diet group from 1 month after starting the diet to termination. No change was observed with the 20 p.p.m. dose in either sex. The average consumption of diet per day per rat by males and females was 15 and 10 g, respectively, with no effects from APNH. All male rats fed the control diet survived to the end of the study, although two control females died of metastasis to lungs from fibrosarcoma and uterus bleeding at 1 week before death. One female and one male rat fed APNH at 40 p.p.m. each developed hepatocellular carcinomas (HCCs) at 49 and 53 weeks, respectively, after starting the study. Some animals fed APNH became moribund and were found to have tumors. Effective numbers of rats were defined as those surviving until week 49 of the study when a HCC was first recognized in a female rat given APNH. At termination, survival rates of rats fed APNH at 20 and 40 p.p.m. were 90 and 48% in males and 73 and 48% in females, respectively.

Tumors induced by APNH

At termination, all surviving animals were killed and necropsies were performed. Details for tumors found in both sexes of rats treated with APNH are summarized in Tables I and II, respectively.

Liver tumors

Both male and female rats fed APNH developed liver tumors, including adenomas and HCCs, which were absent in the controls (Table I). The incidences of liver adenomas were 7 and 18% for male rats fed 20 and 40 p.p.m. of APNH, and 9% for female rats fed 40 p.p.m. of APNH, respectively. In the case of HCCs, the incidences were 10 and 79% for male rats fed 20 and 40 p.p.m. of APNH, and 34% for female rats fed 40 p.p.m. of APNH, respectively. In male rats, most of the APNH-induced HCCs were well differentiated (75%), and 32% were moderately differentiated. Only one tumor was diagnosed as poorly differentiated. On the other hand, all APNH-induced HCCs found in female rats were well differentiated. Among 26 HCCs developed in male rats fed 40 p.p.m. APNH, six cases including two well and four moderately differentiated HCCs demonstrated lung metastasis. Male rats fed APNH at 40 p.p.m. also developed cholangiocellular carcinomas at a 12% incidence. Male rats proved more susceptible to induction of liver tumors than females.

Colon tumors

As shown in Table I, rats fed APNH developed colon adenocarcinomas in a dose-dependent manner (3 and 9% in males and 4 and 13% in females at 20 and 40 p.p.m. APNH, respectively). No colon tumors were found in rats fed the control diet.

Other tumors

The incidences of tumors induced by APNH in organs other than the liver or colon are summarized in Table II. Follicular carcinomas and C-cell carcinomas, in the thyroid gland were observed following APNH administration. The incidence of

Table I. Incidence of liver and colon tumors induced by APNH in F344 rats

Dose of APNH (p.p.m.)	Sex	Effective no. of rats[a]	No. of rats with (%)			
			Liver			Colon
			Adenoma	Hepatocellular carcinoma	Cholangiocellular carcinoma	Adenocarcinoma
0	M	30	0 (0)	0 (0)	0 (0)	0 (0)
	F	30	0 (0)	0 (0)	0 (0)	0 (0)
20	M	30	2 (7)	3 (10)	0 (0)	1 (3)
	F	28	0 (0)	0 (0)	0 (0)	1 (4)
40	M	33	6 (18)[b]	26 (79)[c]	4 (12)	3 (9)[e]
	F	32	3 (9)	11 (34)[d]	0 (0)	4 (13)[c]

[a]Number of rats surviving at 49 weeks, when the first hepatocellular carcinoma was found in a female given 40 p.p.m. of APNH.
[b–d]Significantly different from the control group (0 p.p.m. APNH) by Fisher's exact probability test ([b]$P < 0.05$, [c]$P < 0.00001$, [d]$P < 0.001$).
[e]Numbers of male and female rats combined were significantly different from the control group (0 p.p.m. APNH) by Fisher's exact probability test ($P < 0.05$).

Table II. Incidence of tumors in organs/tissues other than the liver or colon in rats

Dose of APNH (p.p.m.)	Sex	Effective no. of rats[a]	No. of rats with (%)					
			Thyroid				Mononuclear cell leukemia	Clitoral gland carcinoma
			C-cell		Follicular			
			Adenoma	Carcinoma	Adenoma	Carcinoma		
0	M	30	1 (3)	0 (0)	0 (0)	1 (3)	1 (3)	–
	F	30	1 (3)	0 (0)	0 (0)	0 (0)	3 (10)	0 (0)
20	M	30	0 (0)	4 (13)	0 (0)	5 (17)	3 (10)	–
	F	28	1 (3)	0 (0)	0 (0)	1 (4)	9 (32)[b]	3 (10)
40	M	33	1 (3)	2 (6)	1 (3)[e]	5 (15)[e]	11 (33)[d]	–
	F	32	1 (3)	4 (13)	1 (3)[e]	2 (6)[e]	16 (50)[c]	8 (25)[d]

[a]Number of rats surviving at 49 weeks, when the first hepatocellular carcinoma was found in a female given 40 p.p.m. of APNH.
[b–d]Significantly different from control group (0 p.p.m. APNH) by Fisher's exact probability test ([b]$P < 0.05$, [c]$P < 0.001$, [d]$P < 0.01$).
[e]Numbers of male and female rats with follicular adenoma and carcinoma combined were significantly different from the control group (0 p.p.m. APNH) by Fisher's exact probability test ($P < 0.05$).

follicular tumors (adenomas and carcinomas) was significantly increased at 40 p.p.m. APNH group, although there were no apparent effects on incidences of C-cell tumors. Mononuclear cell leukemia was also found in both control and APNH-treated rats, the incidence being significantly increased in a dose-dependent manner. In female rats, clitoral gland carcinomas were induced dose-dependently, incidences being 10 and 25% at 20 and 40 p.p.m. of APNH, respectively.

Transitional cell carcinomas in the urinary bladder were found in a male rat fed 20 p.p.m. of APNH and in two female rats fed 40 p.p.m. of APNH with incidences of 3 and 6%, respectively, although the values were not significantly different from the control group. In males, interstitial cell adenomas of the testes were frequently found in all groups at an incidence of 58–67% incidence, with no obvious influence of APNH. In addition, preputial gland carcinomas, pituitary gland adenomas, lung carcinomas were observed at incidences of 3–7%, without significant deviation from the control group. In female rats, endometrial hyperplasia was found to be increased following APNH feeding (20, 36 and 69% at 0, 20 and 40 p.p.m. of APNH, respectively), but no carcinomas were found.

Genetic alterations in liver and colon tumors induced by APNH

Liver. DNA samples obtained from 17 HCCs were examined for mutations of β-*catenin*, *ras* family, *p53* and *Apc* genes using PCR–SSCP analysis. While no mutations were identified in the H-*ras*, K-*ras*, N-*ras*, *p53* and *Apc* genes, the β-*catenin* gene was found to show mobility-shifted bands in four out of 17 HCC samples (Table III). DNA fragments extracted from those SSCP bands were amplified and subjected to direct sequencing. As shown in Table III, mutations were detected in all four cases: one at the first base of codon 32, two at the second base of codon 37, and one at the second base of codon 41 (a G:C to T:A transversion, C:G to G:C transversions and a C:G to T:A transition, respectively), all leading to amino acid substitutions (Table III).

Table III. Mutation analysis of the β-*catenin* gene in APNH-induced HCCs

Genes	Frequency (%)	Mutation	
		Mutated codon	Mutation pattern
β-*Catenin*	4/17 (24)	32	GAT (Asp) → TAT (Thr)
		37	TCT (Ser) → TGT (Cys)
		37	TCT (Ser) → TGT (Cys)
		41	ACC (Thr) → ATC (Ile)

Mutation analysis were performed by PCR–SSCP and direct sequencing methods.
Primers and PCR conditions were the same as those reported previously (29–34).
No mutations were detected in H-*ras*, K-*ras*, N-*ras*, *p53* or *Apc* genes.

Table IV. Summary of mutation patterns of cancer-related genes in colon adenocarcinomas induced by APNH

Genes	Frequency	Mutated codon	Mutation pattern	Amino acid change
β-*Catenin*	4/9 (44%)	32	GAT → GGT	Asp → Gly
		34	GGA → GAA	Gly → Glu
		34	GGA → AGA	Gly → Arg
K-*ras*	2/9 (22%)	12	GGT → GTT	Gly → Val
Apc	3/9 (33%)	874–875	5′-GGGGTTT-3′ → 5′-GGGTTT-3′	Truncated product (884 aa)
		879	TCT → TCG	Silent
		900	GAC → CAC	Asp → His

Mutation analysis were performed by PCR–SSCP and direct sequencing methods.
Primers and PCR conditions were the same as those reported previously (29–34).
No mutations were detected in H-*ras*, N-*ras* or *p53* genes.

Immunohistochemical analysis of β-catenin indicated that some cancer cells showed prominent immunoreactivity in the nucleus, cytoplasm or cell membrane, whereas non-cancerous hepatocytes lacked β-catenin immunoreactivity in the nucleus and cytoplasm, and showed only weak reactivity, limited to the cell membrane. Accumulation of β-catenin in the nucleus and cytoplasm, compared with the amount seen in non-cancerous hepatocytes, was detected in six of 17 (35%) HCC samples. Among these, five revealed β-catenin accumulation in the cytoplasm, and one in the nucleus. Moreover, four out of six HCC samples showing β-catenin immunoreactivity contained genetic alterations in exon 3 of the β-*catenin* gene.

Colon. The findings of nine cases of colon cancers are summarized in Table IV. Four showed mutations at codons 32 and 34 of the β-*catenin* gene (one A:T to G:C transition at the second base of codon 32, two G:C to A:T transitions at the second base and one G:C to A:T transition at the first base of codon 34), all leading to amino acid changes. In addition, two mutations of K-*ras* and three mutations of *Apc* genes were detected in APNH-induced colon carcinomas. The K-*ras* mutations were G:C to T:A transversions at the second base of codon 12, with change of Gly to Val. Of the three *Apc* mutations detected, one was a frameshift mutation with one G deletion in the 5′-GGGGTTT-3′ sequence resulting in a truncated product, and the other two were base substitutions including one silent (T:A to G:C at codon 879) and one G:C to C:G transversion, leading to amino acid substitution.

Among the colon cancer samples, three had double mutations with K-*ras* and β-*catenin* (two samples) and *Apc* and β-*catenin* (one sample). The *Apc* mutation in the colon tumor sample containing the β-*catenin* mutation was silent. Moreover, all the samples with *Apc* and/or β-*catenin* gene mutation demonstrated strong nuclear or cytoplasmic immunoreactivity with β-catenin. Although PCR–SSCP analyses of H-*ras*, N-*ras* and *p53* genes were performed under at least two conditions, no shifted bands were detected in any of the nine colon carcinomas.

Discussion

Our results indicated clearly that orally administered APNH is carcinogenic in both male and female F344 rats. As expected from our previous finding of GST-P positive liver foci after 4 weeks of treatment (17), the feeding of APNH at 40 p.p.m. for 85 weeks resulted in the development of HCCs at 79 and 34% in male and female F344 rats, respectively, whereas liver tumors were absent in the controls. Most HCCs found in both sexes were well differentiated.

Genetic alteration of β-*catenin* was observed in 24% of the HCCs induced by APNH. However, no mutations were found in *ras* family, *p53* or *Apc* genes. All of the point mutations detected featured replacement of a serine or threonine residue, encoded by codons 37 and 41 or a contiguous site with serine 33 in exon 3, known to be putative phosphorylation targets of GSK-3β. In immunohistochemical analysis, all of the HCCs bearing β-*catenin* gene mutations demonstrated accumulation of β-catenin protein in the nucleus and cytoplasm. In addition, two HCC samples without any mutations showed immunoreactivity. The reason for this is not clear, however, we analyzed only limited regions of β-*catenin* and *Apc* genes; therefore, mutations might occur at other regions of these genes or other wnt signaling related genes. On the other hand, there seems to be no relation between β-catenin accumulation and tumor malignancy. β-Catenin accumulation and mutation of exon 3 have also been reported in diethylnitrosamine-induced rat liver tumors and also in human liver cancers (25–27). With diethylnitrosamine-induced HCCs in rats, mutations were detected in codons 32, 33, 34, 35, 37 and 41 in exon 3 at incidences of 31 and 45% (25,26). In a human series of HCCs, 39% demonstrated accumulation of β-catenin and 24% gene mutations at codons 32, 34, 35, 37 and 41 (27). Thus, the available data suggest that β-*catenin* gene mutations may be related to hepatocarcinogenesis in both rodents and man, although incidences of β-catenin accumulation and gene mutations observed in human and chemically induced HCCs are much lower than in colon cancers. Therefore, pathways rather than β-*catenin*-wnt signaling are presumably involved. Further studies are thus needed to clarify the mechanisms of APNH hepatocarcinogenesis.

As with azoxymethane (AOM)-, 2-amino-3-methylimidazo[4,5-*f*]quinoline (IQ)- and 2-amino-1-methyl-6-phenylimidazo[4,5-*b*]pyridine (PhIP)-induced rat and human colon tumors (21,23,28,29), mutations of β-*catenin*, K-*ras* and *Apc* genes in colon adenocarcinomas were here found to be more frequent than those in HCCs. Missense mutations in K-*ras*, β-*catenin* and *Apc* genes were found in 22, 44 and 33% of the APNH-induced colon tumors, as compared with 62 (K-*ras*), 75 (β-*catenin*) and 8% (*Apc*) in AOM-induced colon tumors (21). The respective figures for the IQ-induced β-*catenin* and *Apc* genes are 100 and 15%, and 57 and 50% for PhIP-induced colon tumors (23,28). In the case of human colon cancers, K-*ras*, β-*catenin* and *Apc* gene mutations have been found in 33–36%, 7–15% and 43–48%, respectively (29). The regions for β-*catenin* gene mutations detected in

APNH-induced colon adenocarcinomas were at codons 32 and 34, which are contiguous with serine 33. These mutations may cause alterations of the β-catenin protein structure, therefore leading to inhibition of phosphorylation of β-*catenin* and blocking of degradation through the ubiquitin–proteasome pathway. In addition, *Apc* gene mutations, except one, led to amino acid change or truncated products, and β-catenin protein accumulation was evident in the APNH-induced colon cancers.

We have reported previously that the structure of the major APNH–DNA adduct was dG-C8-APNH, as is the case with PhIP, IQ and 2-amino-3,8-dimethylimidazo[4,5-*f*]quinoxaline (MeIQx) (14). This adduct has been detected in various organs of rats given 40 p.p.m. APNH for 4 weeks, with levels higher in the liver and colon than in other organs (14). Based on these observations, it is suggested that APNH forms DNA adducts at the C8 position of guanine residues, especially in its target organs. Recently, we have also reported that the *gpt* mutant frequencies were elevated 10- and 5-fold in the liver and colon of the *gpt* delta transgenic mouse treated with 20 p.p.m. APNH, respectively (30). APNH induced G:C to T:A trasversions and single G:C deletions in G:C run sequences predominately in the liver of transgenic mice. Similarly, most gene alterations detected in APNH-induced liver and colon tumors in the present study involved G:C base pairs. From these observations, it is suggested that dG-C8-APNH was formed in the target genes, and these adducts might cause the mutations. Therefore, the mutations detected in the APNH-induced tumors were mainly at G or C (opposite position of G) base pairs.

Development of other tumors, such as thyroid adenocarcinomas, was also found to be enhanced by APNH feeding in both males and females in the present study. Moreover, endometrial hyperplasias were increased by feeding of APNH, and tumors of the hematopoietic system, including leukemia, were found to be enhanced in both sexes. The underlying mechanisms of the development of these tumors by APNH are now under investigation in our laboratory.

In conclusion, APNH demonstrated carcinogenicity in various organs, including the liver and colon, in both sexes of F344 rats, at doses almost 10 times lower than those proved to be carcinogenic for HCAs, such as MeIQx (31). As mentioned above, norharman and aniline are abundantly present in our environment and continuous exposure to both compounds during daily life is conceivable. It is reported that APNH can be detected in the urine of rats administered norharman and aniline (16). Moreover, when 24 h urine samples were collected from smokers and non-smokers and analyzed by LC-MS after purification with HPLC, we found that APNH was clearly detectable in some samples from smokers (own unpublished data). Therefore, it is highly conceivable that APNH is a new type of endogenous mutagen/carcinogen, involved in human carcinogenesis.

It has been reported that norharman is mutagenic in the presence of *o*-toluidine and S9 mix (2,5,32). Moreover, harman (1-methyl-9*H*-pyrido[3,4-*b*]indole), another β-carboline compound, has a similar co-mutagenic activity with aniline or *o*-toluidine (2). Recently, we reported the mutagenic compounds produced by norharman with *o*-toluidine, and harman with aniline or *o*-toluidine, to be 9-(4′-amino-3′-methylphenyl)-9*H*-pyrido[3,4-*b*]indole (amino-3′-methylphenylnorharman, 3′-AMPNH), 9-(4′-aminophenyl)-1-methyl-9*H*-pyrido[3,4-*b*]indole (aminophenylharman, APH) and 9-(4′-amino-3′-methylphenyl)-1-methyl-9*H*-pyrido[3,4-*b*]indole (amino-3′-methylphenylharman, AMPH), respectively (3,33). To clarify the effects of APNH and its derivatives on human health, it is important to further elucidate their detailed biological properties. Furthermore, it is very important to determine how much APNH and its derivatives may be produced in our bodies in daily life, and consider preventive studies in accordance.

Acknowledgements

We thank Drs Kunitoshi Mitsumori, Tokyo University of Agriculture, Hidetaka Sato, Japan Food Research Laboratories and Technology, and Hiroyuki Tsuda, Nagoya City University Medical School, for his helpful advice and discussion on tumor histology and Ms Yurika Teramoto for her expert technical support. This work was supported by Grants-in-Aid for Cancer Research, the Second-Term Comprehensive 10-Year Strategy for Cancer Control from the Ministry of Health, Labour and Welfare, Japan.

References

1. Sugimura,T., Kawachi,T., Nagao,M. *et al.* (1977) Mutagenic principle(s) in tryptophan and phenylalanine pyrolysis products. *Proc. Jpn. Acad.*, **53**, 58–61.
2. Sugimura,T., Nagao,M. and Wakabayashi,K. (1982) Metabolic aspects of the comutagenic action of norharman. In Snyder,R., Jollow,D.J., Parke,D.V., Gibson,C.G., Kocsis,J.J. and Witmer,C.M. (eds), *Biological Reactive Intermediates-II, Chemical Mechanisms and Biological Effects Part B*. Plenum Press, New York and London, pp. 1011–1025.
3. Totsuka,Y., Ushiyama,H., Ishihara,J., Sinha,R., Goto,S., Sugimura,T. and Wakabayashi,K. (1999) Quantification of the co-mutagenic β-carbolines, norharman and harman, in cigarette smoke condensates and cooked foods. *Cancer Lett.*, **143**, 139–143.
4. Ushiyama,H., Oguri,A., Totsuka,Y., Itoh,H., Sugimura,T. and Wakabayashi,K. (1995) Norharman and harman in human urine. *Proc. Jpn. Acad.*, **71B**, 57–60.
5. Nagao,M., Yahagi,T., Honda,M., Seino,Y., Matsushima,T. and Sugimura,T. (1977) Demonstration of mutagenicity of aniline and *o*-toluidine by norharman. *Proc. Japan Acad.*, **53B**, 34–37.
6. Luceri,F., Giuseppe,P., Moneti,G. and Dolara,P. (1993) Primary aromatic amines from side-stream cigarette smoke are common contaminants of indoor air. *Toxicol. Ind. Health*, **9**, 405–413.
7. International Agency for Research on Cancer (IARC) (1982). Aniline and aniline hydrochloride. *IARC Monographs on the Evaluation of Carcinogenic Risks to Humans*. IARC, IARC Scientific Publication, Lyon, **27**, 39–61.
8. Riffelmann,M., Muller,G., Schmieding,W., Popp,W. and Norpoth,K. (1995) Biomonitoring of urinary aromatic amines and arylamine hemoglobin adducts in exposed workers and nonexposed control persons. *Int. Arch. Occup. Environ. Health*, **68**, 36–43.
9. DeBruin,L.S., Pawliszyn,J.B. and Josephy,P.D. (1999) Detection of monocyclic aromatic amines, possible mammary carcinogenesis, in human milk. *Chem. Res. Toxicol.*, **12**, 78–82.
10. Bayoumy,K.E., Donahue,J.M., Hecht,S.S. and Hoffmann,D. (1986) Identification and quantitative determination of aniline and toluidines in human urine. *Cancer Res.*, **46**, 6064–6067.
11. Totsuka,Y., Hada,N., Matsumoto,K., Kawahara,N., Murakami,Y., Yokoyama,Y., Sugimura,T. and Wakabayashi,K. (1998) Structural determination of a mutagenic aminophenylnorharman produced by the co-mutagen norharman with aniline. *Carcinogenesis*, **19**, 1995–2000.
12. Sugimura,T. (1998) A new concept of co-mutagenicity from a phenomenon forgotten for the past two decades: is it more important than previously expected? *Environ. Health Perspect.*, **106**, A522–A523.
13. Totsuka,Y., Takamura-enya,T., Nishigaki,R., Sugimura,T. and Wakabayashi,K. (2004) Mutagens formed from β-carboline with aromatic amines. *J. Chromatogr. B*, **802**, 135–141.
14. Totsuka,Y., Takamura-Enya,T., Kawahara,N., Nishigaki,R., Sugimura,T. and Wakabayashi,K. (2002) Structure of DNA adduct formed with aminophenylnorharman, being responsible for the comutagenic action of norharman with aniline. *Chem. Res. Toxicol.*, **15**, 1288–1294.
15. Ohe,T., Takata,T., Maeda,Y., Totsuka,Y., Hada,N., Matsuoka,A., Tanaka,N. and Wakabayashi,K. (2002) Induction of sister chromatid exchanges and chromosome aberrations in cultured mammalian cells treated with aminophenylnorharman formed by norharman with aniline. *Mutat. Res.*, **515**, 181–188.

16. Totsuka,Y., Kataoka,H., Takamura-Enya,T., Sugimura,T. and Wakabayashi,K. (2002) *In vitro* and *in vivo* formation of aminophenylnorharman from norharman and aniline. *Mutat. Res.*, **506–507**, 49–54.
17. Kawamori,T., Totsuka,Y., Ishihara,J., Uchiya,N., Sugimura,T. and Wakabayashi,K. (2001) Induction of liver preneoplastic lesions by aminophenylnorharman, formed from norharman and aniline, in male F344 rats. *Cancer Lett.*, **163**, 157–161.
18. Boorman,G. A., Eustis,S. L., Elwell,M. R., Montgomery,J. C.A. and MacKenzie,W. F. (eds) (1990) *Pathology of the Fischer Rat*. Academic Press, Inc., San Diego, pp. 1–553.
19. Kudo,M., Ogura,T., Esumi,H. and Sugimura,T. (1991) Mutational activation of c-Ha-ras gene in squamous cell carcinomas of rat Zymbal gland induced by carcinogenic heterocyclic amines. *Mol. Carcinogen.*, **4**, 36–42.
20. Takahashi,M., Minamoto,T., Sugimura,T. and Esumi,H. (1993) High frequency and low specificity of ras gene mutations in rat Zymbal's gland tumors induced by 2-amino-3-methylimidazo[4,5-*f*]quinoline. *Carcinogenesis*, **14**, 1355–1357.
21. Takahashi,M., Fukuda,K., Sugimura,T. and Wakabayashi,K. (1998) Beta-catenin is frequently mutated and demonstrates altered cellular location in azoxymethane-induced rat colon tumors. *Cancer Res.*, **58**, 42–46.
22. Hirayama,Y., Wakazono,K., Yamamoto,M., Kitano,M., Tatematsu,M., Nagao,M., Sugimura,T. and Ushijima,T. (1999) Rare mutations of p53, Ki-ras and beta-catenin genes and absence of K-sam and c-erbB-2 amplification in N-methyl-N'-nitro-N-nitrosoguanidine-induced rat stomach cancers. *Mol. Carcinogenesis*, **25**, 42–47.
23. Kakiuchi,H., Watanabe,M., Ushijima,T., Toyota,M., Imai,K., Weisburger,J. H., Sugimura,T. and Nagao,M. (1995) Specific 5′-GGGA-3′–>5′-GGA-3′ mutation of the Apc gene in rat colon tumors induced by 2-amino-1-methyl-6-phenylimidazo[4,5-*b*]pyridine. *Proc. Natl Acad. Sci. USA*, **92**, 910–914.
24. Ubagai,T., Ochiai,M., Kawamori,T., Imai,H., Sugimura,T., Nagao,M. and Nakagama,H. (2002) Efficient induction of rat large intestinal tumors with a new spectrum of mutations by intermittent administration of 2-amino-1-methyl-6-phenylimidazo[4,5-*b*]pyridine in combination with a high fat diet. *Carcinogenesis*, **23**, 197–200.
25. Yamashita,Y., Yoshimi,N., Sugie,S., Suzui,S., Matsunaga,K., Kawabata,K., Hara,A. and Mori,H. (1999) β-Catenin (*Ctnnb1*) gene mutations in diethylnitrosamine (DEN)-induced liver tumors in male F344 rats. *Jpn. J. Cancer Res.*, **90**, 824–828.
26. Tsujiuchi,T., Tsutsumi,M., Sasaki,Y., Takahama,M. and Konishi,Y. (1999) Different frequencies and patterns of β-catenin mutations in hepatocellular carcinomas induced by *N*-nitrosodiethylamine and a choline-deficient l-amino acid-deficient diet in rats. *Cancer Res.*, **59**, 3904–3907.
27. Kondo,Y., Kanai,Y., Sakamoto,M., Genda,T., Mizokami,M., Ueda,R. and Hirohashi,S. (1999) Beta-catenin accumulation and mutation of exon 3 of the beta-catenin gene in hepatocellular carcinoma. *Jpn. J. Cancer Res.*, **90**, 1301–1309.
28. Dashwood,R.H., Suzui,M., Nakagama,H., Sugimura,T. and Nagao,M. (1998) High frequency of β-*catenin* (*ctnnb1*) mutations in the colon tumors induced by two heterocyclic amines in the F344 rat. *Cancer Res.*, **58**, 1127–1129.
29. Konishi,M., Kikuchi-Yanoshita,R., Tanaka,K. *et al.* (1996) Molecular nature of colon tumors in hereditary nonpolyposis colon cancer, familial polyposis and sporadic colon cancer. *Gastroenterology*, **111**, 307–317.
30. Masumura,K., Totsuka,Y., Wakabayashi,K. and Nohmi,T. (2003) Potent genotoxicity of aminophenylnorharman, formed from non-mutagenic norharman and aniline, in the liver of *gpt* delta transgenic mouse. *Carcinogenesis*, **24**, 1985–1993.
31. Kato,T., Ohgaki,H., Hasegawa,H., Sato,S., Takayama,S. and Sugimura,T. (1988) Carcinogenicity in rats of a mutagenic compound, 2-amino-3, 8-dimethylimidazo[4,5-*f*]quinoxaline. *Carcinogenesis*, **9**, 71–73.
32. Nagao,M., Yahagi,T. and Sugimura,T. (1978) Differences in effects of norharman with various classes of chemical mutagens and amounts of S-9. *Biochem. Biophys. Res. Commun.*, **83**, 373–378.
33. Hada,N., Totsuka,Y., Enya,T., Tsurumaki,K., Nakazawa,M., Kawahara,N., Murakami,Y., Yokoyama,Y., Sugimura,T. and Wakabayashi,K. (2001) Structures of mutagens produced by the co-mutagen norharman with *o*- and *m*-toluidine isomers. *Mutat. Res.*, **493**, 115–126.

Received November 30, 2003; revised May 5, 2004; accepted May 9, 2004

Review Article

Gene mutations and altered gene expression in azoxymethane-induced colon carcinogenesis in rodents

Mami Takahashi and Keiji Wakabayashi

Cancer Prevention Basic Research Project, National Cancer Center Research Institute, 5-1-1 Tsukiji, Chuo-ku, Tokyo 104-0045

(Received February 26, 2004/Revised April 16, 2004/Accepted April 26, 2004)

Studies of colon carcinogenesis in animal models are very useful to elucidate mechanisms and provide pointers to potential prevention approaches in the human situation. In the rat colon carcinogenesis model induced by azoxymethane (AOM), we have documented frequent mutations of specific genes. K-*ras* mutations at codon 12 were found to be frequent in hyperplastic aberrant crypt foci (ACF) and large adenocarcinomas. In addition, mutations of the *β-catenin* gene in its GSK-3β phosphorylation consensus motif could also be identified in many adenomas and adenocarcinomas, and altered cellular localization of β-catenin protein was observed in all of the dysplastic ACF, adenomas and adenocarcinomas examined, indicating that activation of Wnt signaling by accumulation of β-catenin is a major mechanism in the AOM-induced colon carcinogenesis model. Frequent gene mutations of *β-catenin* and altered cellular localization of the protein are also features of AOM-induced colon tumors in mice. Expression of enzymes associated with inflammation, such as inducible nitric oxide synthase (iNOS) and the inducible type of cyclooxygenase (COX), COX-2, is increased in AOM-induced rat colon carcinogenesis, and overproduction of nitric oxide (NO) and prostaglandins is considered to be involved in colon tumor development. We have demonstrated that increased expression of iNOS is an early and important event occurring in step with β-catenin alteration in rat colon carcinogenesis. Activation of K-ras was also found to be involved in up-regulation of iNOS in the presence of inflammatory stimuli. In addition, expression levels of prostaglandin E_2 (PGE_2) receptors may be altered in colon cancers. For example, the EP_1 and EP_2 subtypes have been shown to be up-regulated and EP_3 down-regulated in AOM-induced colon cancers in rats and mice. EP_1 and EP_4 appear to be involved in ACF formation, while alteration in EP_2 and EP_3 is considered to contribute to later steps in colon carcinogenesis. Increased expression of some other gene products, such as the targets of Wnt/β-catenin signaling, have also been reported. The further accumulation of data with this chemically-induced animal colon carcinogenesis model should provide useful information for understanding colorectal neoplasia in man. (Cancer Sci 2004; 95: 475–480)

In recent years, colorectal cancer has increasingly become a major cause of cancer mortality in Japan. Therefore, elucidation of the mechanisms of colon carcinogenesis and the search for chemopreventive agents are important and urgent tasks. Screening of colon cancer preventive agents has been carried out using several *in vivo* animal models, the majority using azoxymethane (AOM), a very potent carcinogen which induces colorectal cancers at high incidence in rats and mice. In relatively short-term experiments, aberrant crypt foci (ACF) induced by treatment with AOM in rats and mice can be used as biomarkers, since the formation and growth of these putative preneoplastic lesions are thought to be useful indices of the effects of carcinogens and agents promoting or preventing carcinogenesis in the colon.[1,2] Recently, other pre-neoplastic lesions such as β-catenin-accumulated crypts and mucin-depleted foci have also been reported as specific biomarkers for colon carcinogenesis.[3–5] Compounds which appear to be effective in the short-term must then be further examined in long-term experiments focusing on AOM-induced colon cancer development. In order to identify novel prevention approaches, it is very important to take into account the mechanisms underlying colon carcinogenesis in this animal model, and this is the rationale for examining mutations in different genes and changes in expression of proteins. Understanding the relationship of such alterations to each step of colon carcinogenesis should help to elucidate the mechanisms of colon carcinogenesis, not only in rodents, but also in humans.

1. Gene mutations in colon carcinogenesis

Colon carcinogenesis is known to be a multistep process involving multiple genetic alterations. Findings for K-*ras*, *APC*, *DCC* and *p53* in tumors are summarized in Table 1. In human lesions, these genes are frequently mutated or deleted.[6–13] K-*ras* and *APC* gene mutations are involved in relative early stages of colon carcinogenesis, while alterations of *DCC* and *p53* are involved in the late stages.[13] K-*ras* mutations are frequent from the ACF stage, while *APC* mutations are frequent from the adenoma stage. Most ACF are hyperplastic and positive for K-*ras* mutations, but about 5% of ACF are dysplastic and harbor *APC* mutations.[9] K-*ras* is an oncogene which encodes an intracellular signaling molecule. Oncogenic mutations in Ras result in constitutive activation of Ras and its downstream signaling pathways, such as the Raf/MEK/MAPK and PI3K/Akt/PKB pathways. The other three are tumor suppressor genes. *DCC* encodes a protein that has homology to cell adhesion molecules, and p53 protein is a transcription factor which regulates the cell cycle and apoptosis. The *APC* gene has been identified as responsible for the inherited colon cancer syndrome adenomatous polyposis coli, the APC protein forming a complex with β-catenin and stimulating its degradation.[14,15] Mutations in the GSK-3β phosphorylation

E-mail: mtakahas@gan2,ncc.go.jp

Abbreviations: AOM, azoxymethane; iNOS, inducible nitric oxide synthase; COX, cyclooxygenase; NO, nitric oxide; ACF, aberrant crypt foci; PGE_2, prostaglandin E_2; MNU, methylnitrosourea; PhIP, 2-amino-1-methyl-6-phenylimidazo[4,5-b]pyridine; SSCP, single strand conformation polymorphism; IL-1β, interleukin-1β; LPS, lipopolysaccharide.

consensus motif of the *β-catenin* gene, as well as *APC* mutations, cause stabilization of β-catenin in the cytoplasm, and induce constitutive transcriptional activation with Tcf-4, a member of the Tcf family of DNA binding proteins.[16, 17] In fact, Sparks *et al.* found mutations of the *β-catenin* gene in half of human colon tumors possessing an intact *APC* gene.[18] In APC-deficient tumors or cell lines, *β-catenin* mutations are generally not detected. It can be concluded that most colon tumors feature change in the APC/ β-catenin/Tcf pathway.

Table 1 also shows gene alterations that occur during chemical carcinogenesis in rat colon. In AOM-induced lesions, K-*ras* mutations are frequent, as seen in human cancers, but *Apc* and *p53* mutations are only rarely observed.[19, 20] This difference can not be explained by species differences, because *p53* mutations have been detected in methylnitrosourea (MNU)-induced rat colon tumors and *Apc* mutations have been found in 2-amino-1-methyl-6-phenylimidazo[4,5-*b*]pyridine (PhIP)-induced tumors.[21, 22] Furthermore, K-*ras* mutation does not appear to be a feature of PhIP-induced colon tumors.[23] The K-*ras* gene is activated by point mutations at codon 12 or 13, while most observed mutations in the *APC* gene in human colon tumors are due to frame-shift deletions or nonsense mutations that produce truncated products. It has also been reported that in the rat, PhIP causes specific one-base deletions of GGGA to GGA in the *Apc* gene.[22] AOM causes point mutations of G:C to A:T transversion type in the K-*ras* gene,[24, 25] which may derive from O^6-methyl-deoxyguanine adducts.[26, 27] Thus, the difference may be carcinogen-specific rather than species-specific. In order to ascertain whether the β-catenin/Tcf pathway is involved in AOM-induced rat colon carcinogenesis, we have focused on β-catenin in AOM-induced rat colon tumors, and we found frequent mutations and altered cellular localization.[28, 29] *β-Catenin* mutations have also been found in PhIP-induced rat colon tumors without *Apc* mutations.[30] These results indicate that Wnt/Apc/β-catenin signaling indeed plays important roles in chemically-induced rat colon carcinogenesis, as it does human cancers.

1.1 β-Catenin

Male F344 rats were treated with AOM to induce colon tumors, and adenocarcinomas obtained after 36 weeks were examined by PCR-single strand conformation polymorphism (SSCP) analysis and direct sequencing for *β-catenin* mutations in the GSK-3β phosphorylation consensus motif. Immunohistochemical staining and immunoblotting were also performed to examine the cellular localization and protein level, with an additional focus on small adenomas and ACF to investigate alteration of the β-catenin pathway in different steps of colon carcinogenesis.[29]

Fig. 1 shows the DNA sequence around the GSK-3β phosphorylation consensus motif of rat β-catenin. The *β-catenin* mutations found in our study were located in codons 33 and 41, which are encode serine and threonine residues important for GSK-3β phosphorylation, and in codons 32 and 34, encoding

Table 1. Gene alterations in colon cancers

Species	Carcinogen	Lesion	Mutation frequency (%)				
			APC	*β-Catenin*	*K-ras*	*DCC*	*p53*
Human		Adenocarcinoma	40–80	15	40–60	40–70	50–80
		Adenoma	40–65	—	0–40	—	—
		ACF	<5	—	10–95	—	—
Rat	AOM	Adenocarcinoma	8	75	30–60	—	0
		ACF	0	—	20–40	—	0
	PhIP	Adenocarcinoma	13	50	0	—	0
	MNU	Adenocarcinoma	—	—	18	—	27
Mouse	AOM	Adenocarcinoma	—	100	0–10	—	0

References: 6–13, 18–25, 28, 30, 32).
—: No data.

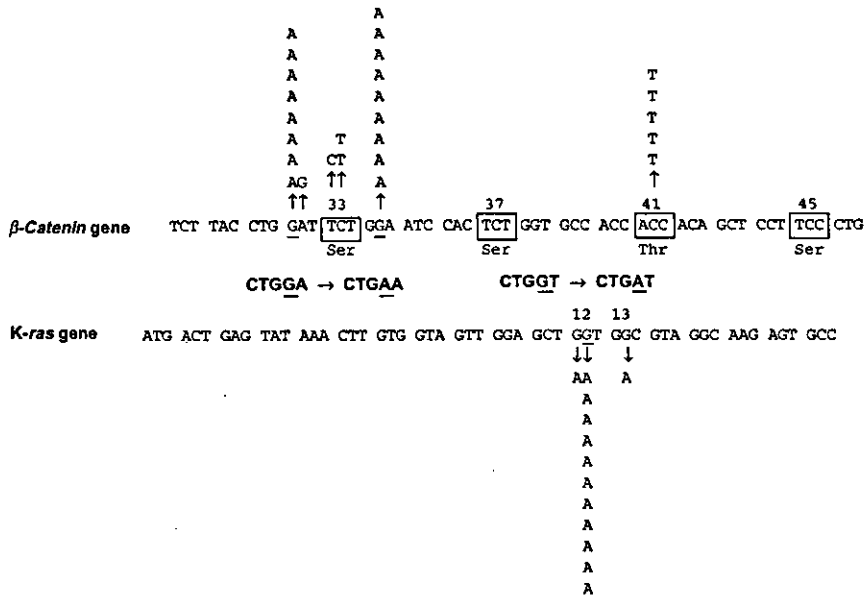

Fig. 1. Mutations of the *β-catenin* and *K-ras* genes in rat colon lesions induced by AOM. The serine residues encoded by codons 33, 37 and 45 and the threonine residue encoded by codon 41 of the *β-catenin* gene are GSK-3β phosphorylation sites. Mutational hot spots are the second G of CTGGA/T sequences, indicated in red.

Table 2. Alterations in AOM-induced colonic lesions in rats[1]

Gene or protein	Alteration	Frequency (%) in				
		Hyperplastic ACF	Dysplastic ACF	Adenoma	Small adenocarcinoma[2]	Large adenocarcinoma[3]
K-ras	Mutation	70	0	0	8	43
β-Catenin	Mutation	0	66	33	75	79
β-Catenin	Cytoplasmic & nuclear translocation	0	100	100	100	100
iNOS	Increased expression					
	in epithelial cells	0	100	100	92	100
	in stromal cells	−	−	−	−	±
COX-2	Increased expression					
	in epithelial cells	0	0	17	42	79
	in stromal cells	+	+	++	++	+++

1) Reference: 29).
2) Small adenocarcinomas: 1–5 mm.
3) Large adenocarcinomas: >5 mm.

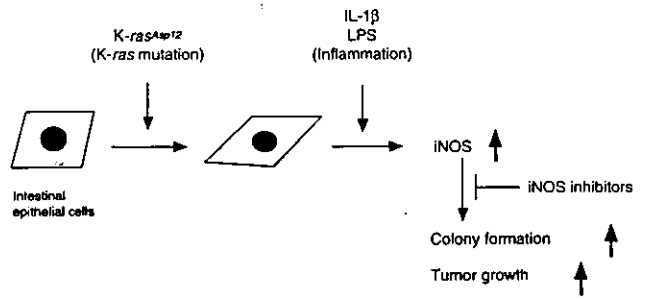

Fig. 2. K-*ras* codon 12 mutations can elevate iNOS expression mediated by IL-1β and LPS. Rat intestinal epithelial cells (IEC-6) were transfected with K-*ras*^{Asp12} mutant cDNA. In the presence of IL-1β or LPS stimuli, iNOS expression is markedly enhanced, and anchorage-independent growth is elevated. Note suppression of the *in vivo* growth of IEC-6/K-*ras*^{Asp12} cells by NOS inhibitors.

residues adjacent to the serine residue encoded by codon 33, and presumably affecting its phosphorylation. Frequent mutations in codons 32 and 34 are CTGGA to CTGAA. The common K- and H-*ras* mutations in codon 12 that have been observed frequently in AOM-induced rat colon tumors are also CTGGT to CTGAT, and CTGGA to CTGAA, respectively.[24, 25, 29, 31] Thus, the second G in CTGGA or CTGGT sequences may be a hot spot for AOM-induced mutations. As shown in Table 2, mutations in the *β-catenin* gene were found to be frequent from the step of dysplastic ACF.[29]

In normal colon epithelium, β-catenin exists mainly as a component of the cadherin-mediated cell-cell adhesion system and is immunohistochemically stained at the cellular membrane. In contrast, pronounced cytoplasmic and nuclear staining of β-catenin was seen in all AOM-induced colon adenocarcinomas examined. As summarized in Table 2, alteration of the cellular localization of β-catenin was observed in all dysplastic ACF, adenomas and adenocarcinomas examined, but not in any hyperplastic ACF.[29] These results indicate the importance of dysplastic ACF as a precursor of colon cancer.

Analysis of mutations in the *β-catenin* gene and altered cellular localization in mouse colon carcinomas induced by AOM yielded similar results to those found in the rat. A hot-spot in the mouse *β-catenin* gene was found in codon 34 at the second G of the CTGGA sequence. Other mutations were identified in codons 33, 41 and 37, but not codon 32. In addition to the nuclear staining of β-catenin with a scattered heterogeneous pattern, which is common to the rat, mouse-distinctive homogeneous or focal heterogeneous nuclear staining was evident.[32] Furthermore, reduced expression of Apc protein in AOM-induced mouse tumors has been reported.[33] The results show that β-catenin alterations are early events in AOM-induced colon tumorigenesis, and may play important roles in causing dysplastic changes.

1.2 K-ras

Using the same DNA samples employed for the mutation analysis of the *β-catenin* gene, rat K-*ras* gene mutations were analyzed. Fig. 1 shows mutations detected in exon 1. All were G:C to A:T transitions, and the most frequent was CTGGT to CTGAT at the second base of codon 12. As shown in Table 2, in the AOM-induced rat colon carcinogenesis model, K-*ras* activating mutations at codon 12 were very frequently observed in ACF and tumors, especially in large tumors, as in human cancers, indicating that activation of K-ras may be involved in promotion of cell proliferation.[29] On the other hand, K-*ras* mutations in mouse colon carcinomas induced by AOM proved rare.[32] It has also been reported that K-*ras* mutations are not detected in mouse colon tumors induced by 1,2-dimethylhydrazine, a precursor of AOM.[34] These findings suggest that activation of the K-*ras* gene is not essential for colon cancer development.

2. Altered gene expression in colon carcinogenesis

In human colorectal cancers, the expression of enzymes associated with inflammation, such as inducible nitric oxide synthase (iNOS) and inducible-type cyclooxygenase, COX-2, have been reported to be elevated,[35, 36] and their reaction products, nitric oxide (NO) and prostaglandin E_2 (PGE_2), could contribute to colon tumorigenesis. However, the relation between their expression and gene alteration remains to be clarified .

In our studies of the expression of iNOS and COX-2 in AOM-induced rat colorectal cancers by immunoblotting and immunohistochemical staining, the levels of both proteins were found to be markedly elevated.[29, 37]

2.1 iNOS

In normal colon mucosa, iNOS expression is hardly detectable in epithelial or stromal cells. As summarized in Table 2, increased expression of iNOS in epithelial cells is very frequently observed in dysplastic ACF, adenomas and adenocarcinomas, but not in hyperplastic ACF. Thus, iNOS expression is detected in almost all lesions in which β-catenin alterations are observed, indicating a possible direct or indirect causal relationship. However, iNOS expression within tumors was not homogeneous, in contrast to the β-catenin alteration.[29] Positive